Further Bounding the Kreuzer-Skarke Landscape

Nate MacFadden [a], Stepan Orevkov,[b] and Michael Stepniczka [a]

[a] *Department of Physics, Cornell University, Ithaca, New York 14853 USA*
[b] *Institut de Mathématiques de Toulouse, Université de Toulouse, Toulouse 13062 France*

nate.macfadden@gmail.com, stepan.orevkov@math.univ-toulouse.fr, ms3296@cornell.edu

Abstract

Batyrev's construction provides a map from fine, regular, star triangulations (FRSTs) of 4D reflexive polytopes to smooth Calabi-Yau threefolds (CYs). We prove that there are at most 10^{296} diffeomorphism classes of CYs produced in this manner, improving [1]'s upper bound of 10^{428}. To show this, we make use of the fact that any two FRSTs with the same 2-face restrictions give rise to diffeomorphic CYs and bound the number of such '2-face equivalence classes' for all polytopes with Hodge number $h^{1,1} \geq 300$. We also put a lower bound of 10^{276} on the number of 2-face equivalence classes, but emphasize that this is not a lower bound on the number of diffeomorphism classes of CYs, as distinct 2-face equivalence classes may give rise to diffeomorphic threefolds.

Contents

1 Introduction

This paper concerns the number of distinct 4D effective field theories defined as compactifications of string theory over smooth Calabi-Yau threefolds (CYs). Since non-diffeomorphic threefolds give rise to physically inequivalent effective field theories, one is interested in the count of diffeomorphism classes of CYs. Precisely counting the number of such classes is an active area of research, with current methods only applying to a small subset of known CYs [2,3]. Rather than furthering this precise count, we follow [1] and substantially tighten the best-known *bounds* on the number of diffeomorphism classes of CYs that are producible via Batyrev's construction [4].

The motivation for studying such CYs is that they are both the most numerous across any known construction and they are remarkably accessible. The accessibility is due to the combinatorial nature of Batyrev's construction, which, for our purposes, defines a smooth Calabi-Yau threefold from the data of a triangulation (satisfying various properties – see Section 1.1) of any 4D reflexive polytope. Recall that a polytope is called *reflexive* if it is lattice and its polar dual is also lattice. All 473,800,776 such 4D reflexive polytopes were enumerated by Kreuzer and Skarke in what is known as the Kreuzer-Skarke database [5], and can be retrieved on-demand. Triangulations are well suited for computer-based studies, so these CYs can be understood efficiently via the use of combinatorial, triangulation-focused algorithms. For example, using the software package `CYTools` [6], researchers routinely study millions of such CYs in the scope of a paper. Together, then, the abundance and accessibility of these CYs make them one of the most exciting frameworks for constructing effective theories of quantum gravity – see [7–9] for some example studies.

Upper bounds on the number of diffeomorphism classes of CYs producible via Batyrev's construction were originally obtained in [1], whereby bounding the number of relevant triangulations, it was demonstrated that there are at most 10^{928} such classes. In the same paper, the authors then made use of Wall's theorem [10] to substantially tighten the upper bound by 500 orders of magnitude to 10^{428}. This theorem, as further discussed in Section 1.1, implies that two such CYs are diffeomorphic if their underlying triangulations have identical 2-face restrictions. In this way, one defines equivalence classes of triangulations which we call '2-face equivalence classes'. Clearly, then,

$$\#\text{ diffeomorphism classes of CYs} \leq \#\text{ 2-face equivalence classes.} \tag{1.1}$$

To obtain the improved upper bound of 10^{428}, the authors of [1] bounded the number of 2-face equivalence classes from above. Prior to this work, it was unknown how loose this upper bound of 2-face equivalence classes was; in this work, we strengthen it to 10^{296}, and furthermore, show that it cannot drop beneath 10^{276}. We nevertheless stress: a lower bound on the number of 2-face equivalence classes is *not* a lower bound on the number of diffeomorphism classes of CYs, as two CYs with distinct 2-face restrictions can be diffeomorphic[1].

Out of the ∼half-billion 4D reflexive polytopes, only a handful of them support a non-negligible count of 2-face equivalence classes (and hence, only this handful can potentially support a non-negligible count of CYs). In particular, the best prior bound on the number of 2-face equivalence classes depends (roughly) exponentially on the Hodge number $h^{1,1}$.

[1] In fact, to the best of the authors' knowledge, a non-trivial lower bound on the number of diffeomorphism classes of CYs arising from Batyrev's construction is not known, beyond direct enumeration at small Hodge number $h^{1,1}$.

This is most apparent when comparing the unique polytope with the maximal value $h^{1,1} = 491$,

$$\Delta^\circ_{491} \coloneqq \text{conv}\begin{pmatrix} -63 & 0 & 0 & 1 & 21 \\ -56 & 0 & 1 & 0 & 28 \\ -48 & 1 & 0 & 0 & 36 \\ -42 & 0 & 0 & 0 & 42 \end{pmatrix}, \tag{1.2}$$

to all others ($h^{1,1} \leq 462$) in [1]'s bounds: while Δ°_{491} supports at most 10^{428} 2-face equivalence classes, all other polytopes together support only at most 10^{402} 2-face equivalence classes. To improve bounds on the count of distinct CYs, then, it suffices to limit attention to the largest $h^{1,1}$ polytopes. It is for this reason that we study all 4D reflexive polytopes with $h^{1,1} \geq 300$ in this paper, although we note that the methods utilized in this work are relevant to any polytope. In particular, we will use Δ°_{491} as a running example.

To build up to our improved bound of 10^{296}, we first recall Batyrev's construction, Wall's theorem, and 2-face equivalence classes in Section 1.1. With this background covered, we then demonstrate in Section 2 how to reduce the upper bound on the number of distinct CYs. Finally, we demonstrate a lower-bound of such 2-face equivalence classes in Section 3 that is only ~ 20 orders of magnitude from the upper bound. We conclude in Section 4.

1.1 Review of FRSTs and Wall's theorem

To understand Batyrev's construction [4] to the level necessary to count the corresponding CYs, we first must review triangulations. Let P be a convex lattice polytope and, following [1], let $F_P(d)$ denote its collection of d-dimensional faces. By a 'triangulation' of P, we mean[2] a simplicial complex subdividing P with vertices taken from $P \cap \mathbb{Z}^4$.

The polytopes of interest for Batyrev's construction are 4D reflexive polytopes – denote them as Δ°. While one can use all points $\Delta^\circ \cap \mathbb{Z}^4$ in their triangulations, it is beneficial to further restrict vertices to

$$\mathbf{A}(\Delta^\circ) \coloneqq \{p \in \Delta^\circ \cap \mathbb{Z}^4 : p \notin \text{relint}(f) \text{ for all } f \in F_{\Delta^\circ}(3)\} \tag{1.3}$$

for such reflexive polytopes. In other words, one discards any lattice points strictly interior to facets. This restriction is useful because (see, e.g., Appendix B of [13]) points strictly interior to facets of Δ° do not affect the resulting CY and because every triangulation $\mathcal{T}'$ defined over $\Delta^\circ \cap \mathbb{Z}^4$ has a '2-face equivalent' triangulation $\mathcal{T}$ defined over $\mathbf{A}(\Delta^\circ)$ [1]. See [14] for such a map $\mathcal{T}' \to \mathcal{T}$. Thus, no diffeomorphism classes are missed by such a restriction. The restriction can be thought of as simplifying the polytope by discarding 'irrelevant' points.

Label the points $\mathbf{A} = \{p_1, \ldots, p_N\}$. For a triangulation $\mathcal{T}$ of Δ° to be suitable for Batyrev's construction, it must also satisfy the following three properties:

1. $\mathcal{T}$ is *fine*, i.e. every point $p \in \mathbf{A}$ is the vertex of at least one simplex[3] $\sigma \in \mathcal{T}$,
2. $\mathcal{T}$ is *regular*, i.e. it can be obtained as the lower faces of conv $(\{(p_i, \omega_i) : 1 \leq i \leq |\mathbf{A}|\})$ for some 'heights' $\omega = (\omega_1, \ldots, \omega_N)$ (see Figure 1), and
3. $\mathcal{T}$ is *star*, i.e. the unique lattice point $p \in \text{int}(\Delta^\circ)$ (typically taken to be the origin) is a vertex of every 4-simplex $\sigma \in \mathcal{T}$.

[2]This definition can actually be generalized – see e.g. [11, 12]

[3]N.B.: for 2D lattice polygons, 'fine' is synonymous with 'unimodular' or 'primitive'.

If $\mathcal{T}$ is fine, regular, and star, we call it an 'FRST'; if $\mathcal{T}$ only obeys a subset of the properties, then only the corresponding letters are kept. Note, these properties can directly be generalized to any convex polytope P, with the caveat that the 'star' property only makes sense if P has a unique interior point.

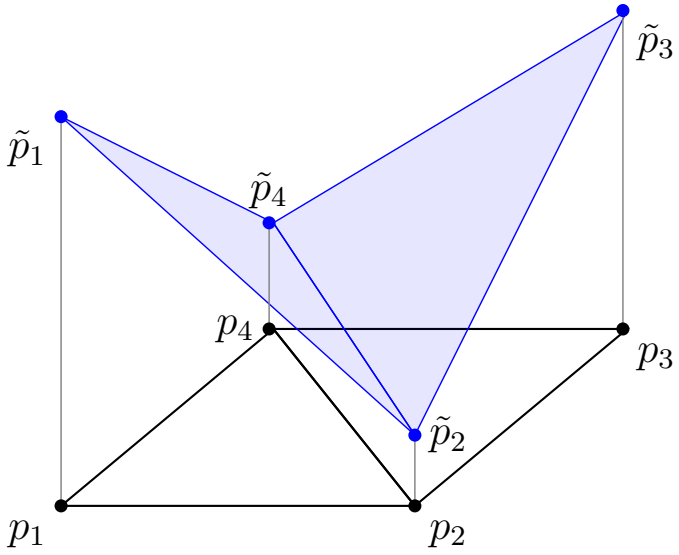

Figure 1: Diagram of the 'lifting' procedure defining regular triangulations. The points p_1, p_2, p_3, and p_4 are embedded into $\mathbb{R}^3$ and then lifted by heights $\omega_1 = 1.1$, $\omega_2 = 0.2$, $\omega_3 = 0.9$, and $\omega_4 = 0.3$. The convex hull of the lifted point configuration is a 3-simplex whose lower faces are plotted in blue. Projecting out the lifted coordinate generates the regular triangulation plotted in black. Figure modified from [14].

With this terminology, we now recall Batyrev's construction [4]. Consider an FRST $\mathcal{T}$ of a 4D reflexive polytope Δ°. Since $\mathcal{T}$ is star, it defines a complete simplicial fan and hence a toric variety. Additionally, since $\mathcal{T}$ is regular, this toric variety is projective and hence Kähler. Batyrev's construction, then, is the identification of (the closure of) a generic anticanonical hypersurface of this toric variety as a (potentially singular) Calabi-Yau threefold. This hypersurface is given by $F = 0$, where the polynomial F is implicitly defined to have a Newton polytope dual to Δ°. In fact, since $\mathcal{T}$ is also fine, the singularities of the toric variety are sufficiently mild such that the CY is smooth[4]. Since there are $\leq 10^{928}$ FRSTs of 4D reflexive polytopes [1], there are naïvely $\leq 10^{928}$ such CYs.

For example, the dual polytope of Δ°_{491} is

$$\text{conv}\begin{pmatrix} -1 & -1 & -1 & -1 & 1 \\ -1 & -1 & -1 & 2 & -1 \\ -1 & -1 & 6 & -1 & -1 \\ 2 & 4 & -4 & 0 & 1 \end{pmatrix},$$

[4]By [4], this smoothness relies on the dimension of the reflexive polytope being ≤ 4; otherwise, this procedure may not resolve all singularities intersecting a generic Calabi-Yau hypersurface.

and thus the associated CYs are closures of generic hypersurfaces of the form

$$\begin{aligned}
&c_0 + c_1\frac{y}{x} + c_2\frac{z}{x} + c_3\frac{z}{y} + c_4\frac{w}{x} + c_5\frac{w}{y} + c_6\frac{w}{z} \\
&+ c_7\frac{y^2}{xz} + c_8\frac{z^2}{xy} + +c_9\frac{z^2}{xw} + c_{10}\frac{z^2}{yw} + c_{11}\frac{w^2}{xy} + c_{12}\frac{w^2}{xz} + c_{13}\frac{w^2}{yz} \\
&+ c_{14}\frac{xw}{yz} + c_{15}\frac{yz}{xw} + c_{16}\frac{yw}{xz} + c_{17}\frac{zw}{xy} + c_{18}\frac{z^3}{xw^2} \\
&+ c_{19}\frac{z^3}{xyw} + c_{20}\frac{z^4}{xyw^2} + c_{21}\frac{z^5}{xyw^3} + c_{22}\frac{z^6}{xyw^4} + c_{23}\frac{w^2}{xyz} + c_{24}\frac{w^3}{xyz} + c_{25}\frac{w^4}{xyz} = 0.
\end{aligned}$$

While the bound on FRSTs is directly a bound on the number of diffeomorphism classes of CYs, Wall's theorem [10] enabled [1] to make stronger statements about when two FRSTs define equivalent CYs. Wall's theorem states that the diffeomorphism classes of such (simply connected, torsion-free) CYs[5] are determined by their Hodge numbers, second Chern class, and triple intersection numbers. As is discussed in [1], the Hodge numbers are determined by the underlying polytope, while the second Chern class and intersection numbers are determined by the 2-face restrictions of the triangulation. Thus, if two FRSTs $\mathcal{T}_1$ and $\mathcal{T}_2$ of the same polytope Δ° have the same 2-face restrictions, then their associated CYs are diffeomorphic. It is therefore convenient to define an equivalence relation such that $\mathcal{T}_1 \sim \mathcal{T}_2$ if and only if $\mathcal{T}_1$ has the same 2-face restrictions as $\mathcal{T}_2$ (i.e., if their 2-skeletons have the same triangulations); denote this as '2-face equivalence'[6].

In this language, we are interested in the count of 2-face equivalence classes coming from all polytopes in the Kreuzer-Skarke database. [1] demonstrated that this quantity is at most 10^{428}. The leading contribution comes from 2-face equivalence classes of Δ°_{491}; the rest of the Kreuzer-Skarke polytopes together contribute 10^{402} to this bound. In the present paper, we show that the number of 2-face equivalence classes of Δ°_{491} is still the leading contribution, with a true count bounded between 10^{276} and 10^{296}. Moreover, we show that the rest of the polytopes together contribute at most 10^{279} to this bound. We leave it to future work to apply this to all Kreuzer-Skarke polytopes.

2 Upper Bounds

For a given polytope Δ°, each 2-face equivalence class is defined by the fine, regular triangulations (i.e., FRTs) of the 2-faces $f \in F_{\Delta^\circ}(2)$. However, as will be further discussed in Section 3, not every collection of FRTs of 2-faces can be realized as simultaneously descending from any FRST. Thus, the number of 2-face equivalence classes defined by Δ° is bounded by the number of distinct ways to assign FRTs to these 2-faces:

$$\#\text{2-face equivalence classes of } \Delta^\circ \leq \prod_{f \in F_{\Delta^\circ}(2)} N_{\text{FRT}}(f). \tag{2.1}$$

To bound the number of 2-face equivalence classes, it then suffices to evaluate $N_{\text{FRT}}(f)$ for each 2-face f of Δ°. Unfortunately, it is generally computationally expensive to count the number of FRTs for a lattice polygon. Fortunately, most 2-faces arising in the Kreuzer-Skarke database are sufficiently small for the cost to be negligible. For instance,

[5]Note, in [15], Batyrev and Kreuzer find 16 mirror pairs of 4D reflexive polytopes which fail these conditions, meaning Wall's theorem does not apply. None of these polytopes appear in the collection considered in this work, i.e. those with $h^{1,1} \geq 300$.

[6]One can also ask for 2-face equivalence up to polytope automorphism. As Δ°_{491} has the largest count of 2-face equivalence classes but only has two automorphisms, we do not consider this.

despite having a moderately high $h^{1,1} = 60$ and a sizable bound of at most 10^{36} 2-face equivalence classes, the example in Section 4.2 of [16] has $N_{\text{FRT}}(f) \leq 724$ for all of its 2-faces. Said polytope generates this upper bound not via large 2-faces, but instead via many 2-faces each with a moderate number of FRTs.

In contrast, [1]'s bound on 2-face equivalence classes is dominated by Δ°_{491} despite it having only ten 2-faces, the minimum possible number of faces in 4D. This is possible because three of its 2-faces, f_8, f_9, and f_{10} are considerably large and therefore admit many FRTs – see Table 1. These 2-faces each have enough FRTs such that directly counting them is generally computationally infeasible, primarily due to checking regularity. Nevertheless, we *are* able to determine the exact number of FRTs of f_8 because, as will be discussed in Section 3, every fine triangulation of f_8 is also regular. However, for f_9 and f_{10}, current algorithms for counting N_{FRT} would involve enumerating all FTs and then checking the regularity of each triangulation. Regularity can be checked by solving a linear feasibility problem $Hx > 0$ for x, where H is a matrix determined by the simplices of each triangulation. Needless to say, it is computationally infeasible to solve e.g. $\geq 10^{180}$ such problems.

2-face	affinely equivalent polygon	FRT lower bound	FRT upper bound
f_1	$\text{conv}\begin{pmatrix}0&1&0\\0&0&1\end{pmatrix}$	1	1
f_2, f_3	$\text{conv}\begin{pmatrix}0&2&0\\0&0&3\end{pmatrix}$	5	5
f_4, f_5	$\text{conv}\begin{pmatrix}0&2&0\\0&0&7\end{pmatrix}$	204	204
f_6, f_7	$\text{conv}\begin{pmatrix}0&3&0\\0&0&7\end{pmatrix}$	19594	19594
f_8	$\text{conv}\begin{pmatrix}0&2&0\\0&0&84\end{pmatrix}$	2.02×10^{35}	2.02×10^{35}
f_9	$\text{conv}\begin{pmatrix}0&3&0\\0&0&84\end{pmatrix}$	8.73×10^{61}	7.61×10^{65}
f_{10}	$\text{conv}\begin{pmatrix}0&7&0\\0&0&84\end{pmatrix}$	3.90×10^{167}	1.96×10^{180}

Table 1: Affinely equivalent polygons to the 2-faces of Δ°_{491}. Both lower bounds and upper bounds on the number of fine regular triangulations (FRTs) of each 2-face are cited.

Fortunately, while it is desirable to use counts N_{FRT} in (2.1), we can also use upper bounds of these counts. This was the exact strategy used in [1] to bound $N_{\text{CY}} \leq 10^{428}$, for which the authors used exact counts $N_{\text{FRT}}(f)$ for faces $f_1, \ldots, f_7$ and Anclin's upper bound[7] [19] on N_{FT} for f_8, f_9, and f_{10}. As there is no practical algorithm for determining N_{FRT} for such polygons, when the counts of N_{FRT} are inaccessible, we instead make improvements by utilizing the general methods of [20, 21] to evaluate N_{FT} exactly[8]. See

[7] A stronger bound for lattice rectangles exists [17, 18] which can be adapted to other lattice polygons.

[8] We note that in [1], the authors used N_{FRT} rather than N_{FT} for 2-faces with at most 17 lattice points. While we include these data when relevant in Appendix E, to the precision reported in our bounds below, these differences do not matter. Therefore, should one wish, one may replace the inequality (2.1) with $N_{\text{FT}}(f)$ for all 2-faces f.

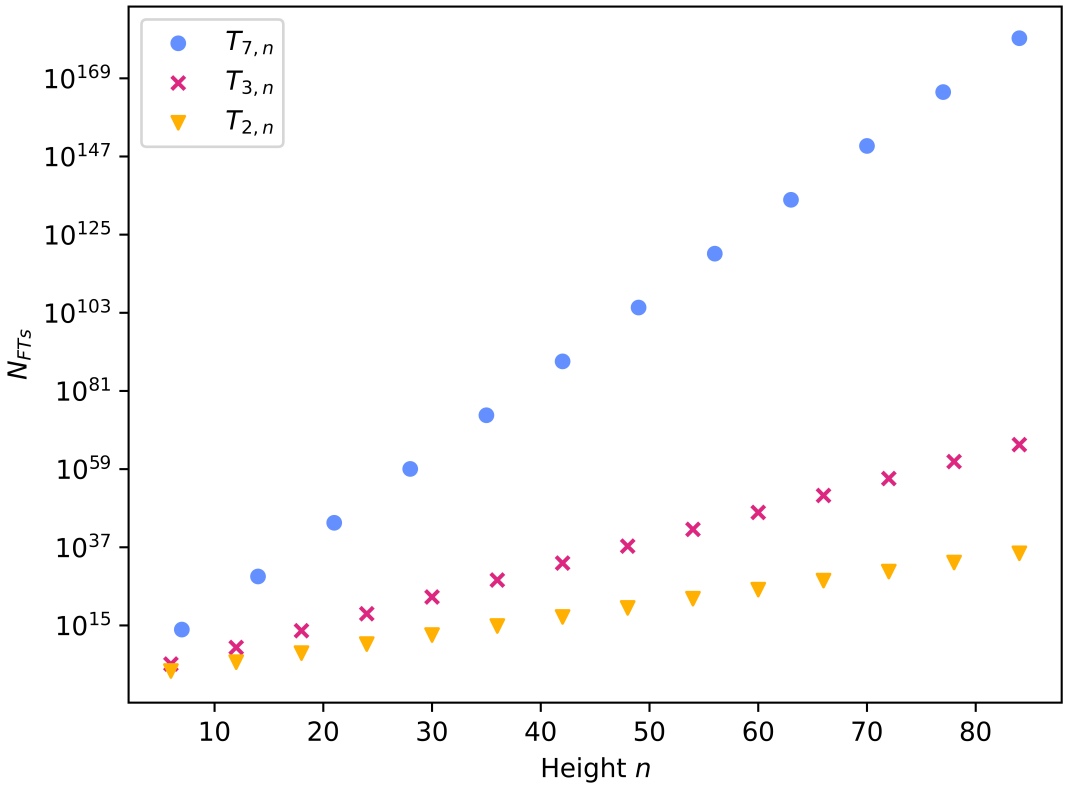

Figure 2: The number of fine triangulations of right lattice triangles $T_{2,n}, T_{3,n}$, and $T_{7,n}$ as a function of the height n. In particular, $T_{2,84}$, $T_{3,84}$, and $T_{7,84}$ correspond to f_8, f_9, and f_{10} respectively.

Appendices B and C for more details regarding the algorithm.

Specifically, our procedure for evaluating $N_{\mathrm{FT}}(f)$ for the 2-faces f is:

1. select the largest N prime numbers ≤ 32767 such that their product is larger than Anclin's bound on $N_{\mathrm{FT}}(f)$, thus enabling use of the Chinese Remainder Theorem,
2. evaluate, using the methods of [21], $N_{\mathrm{FT}}(f) \bmod p$ for each prime number, and then
3. combine the computations using the Chinese Remainder Theorem to evaluate $N_{\mathrm{FT}}(f)$.

Our selection of primes ensures that all counts appearing in the computation can be stored as 16-bit integers[9]. This measure is necessary because, even with just 16-bit integers, each computation required a significant $\mathcal{O}(40\mathrm{GB})$ RAM. Note that since the time of performing the initial computations, the `C` code has been improved to use 32-bit offsets rather than 64-bit pointers and has been parallelized [22, 23]. The memory usage can be further optimized if we restrict our focus to a specific geometry, e.g. to right lattice triangles. However, while this would suffice for studying Δ°_{491}, it would not suffice for studying the set of 2-faces arising from all Kreuzer-Skarke polytopes with $h^{1,1} \geq 300$.

[9] In hindsight, we note that *unsigned* 16-bit integers allows one to use primes up to $2^{16} - 1 = 65535$.

2.1 Example: upper bounds for Δ°_{491}

We now compute the precise number of fine triangulations for the large 2-faces of Δ°_{491}. Take, for example, f_{10}. This 2-face had the largest value for Anclin's bound, $N_{\text{FT}}(f_{10}) < 10^{251}$. Thus, the following $n = 57$ primes were used to obtain the correct result.

$$10^{251} \leq \prod_{i=1}^{n} p_i = 29443 \times \cdots \times 30109. \tag{2.2}$$

Running the computation over each fixed prime (without parallelization) took $\mathcal{O}(1 \text{ day})$ using an Apple Silicon M1 Max chip. Given the magnitude of this computation, we record $N_{\text{FT}}(f_{10})$ as well as some intermediate counts in Figure 2 and Table 2. We find $N_{\text{FT}}(f_{10}) \approx 10^{180}$ which is 70 orders of magnitude smaller than Anclin's bound. Likewise, we applied this algorithm to f_8 and f_9, resulting in counts of $N_{\text{FT}}(f_8) \approx 10^{35}$ and $N_{\text{FT}}(f_9) \approx 10^{66}$, respectively. See Table 3. Combining the results of Table 3 in (2.1), using $N_{\text{FRT}}(f)$ and $N_{\text{FT}}(f)$ as applicable, gives us:

$$N_{\text{CY}}^{\Delta^\circ_{491}} < 1.21 \times 10^{296}. \tag{2.3}$$

In Appendix A, we also provide an alternative recursive formula (A.2) which suffices for f_8. This formula is a generalization of other results in [20] and is possible because the small width of the face f_8 lends itself easily to direct analysis.

2.2 Upper bounds for Kreuzer-Skarke

We repeat analogous computations and find the number of fine triangulations for the 2-faces of all 400 other polytopes with $h^{1,1} \geq 300$. Up to affine equivalence, there are an additional 326 such distinct 2-faces, and all of their counts of fine triangulations can be seen in Appendix E. Putting these data together using (2.1), we find:

$$\sum_{\substack{\text{4D reflexive polytopes } \Delta^\circ \\ \text{with } 300 \leq h^{1,1} < 491}} N_{\text{CY}}^{\Delta^\circ} < 6.89 \times 10^{278}. \tag{2.4}$$

In particular, looking at Figure 3, we see that the bounds for all polytopes with $h^{1,1} \geq 300$ still appear to approximately follow an exponential trend in $h^{1,1}$, with Δ°_{491} dominating by roughly 20 orders of magnitude.

To determine an upper bound on all Kreuzer-Skarke polytopes, we then make use of the data obtained in [1]. Specifically, we take their exact upper bound on all of KS (found in footnote 8 of [1]), and compute the upper bounds as described in their paper for all polytopes with $h^{1,1} \geq 300$. Taking the difference then leaves us with:

$$\sum_{\substack{\text{4D reflexive polytopes} \\ \Delta^\circ \text{with } h^{1,1} < 300}} N_{\text{CY}}^{\Delta^\circ} < 9.33 \times 10^{258}. \tag{2.5}$$

As this is roughly 40 orders of magnitude smaller than (2.3), we leave it to future work to compute tighter bounds for these polytopes and show that they follow the trend of Figure 3.

Equations (2.3) to (2.5) altogether give our main result:

$$N_{\text{CY}}^{\text{KS}} < 1.211 \times 10^{296}. \tag{2.6}$$

n	# fine triangulations of $T_{7,n}$	magnitude
7	72977202065037	7.29×10^{13}
14	673038593104450305321437354 47	6.73×10^{28}
21	825382418330716623196080770138314741803791 71	8.25×10^{43}
28	110469482551636815834083564970273245813170066131344202994021	1.10×10^{59}
35	153405520601065827395233041403916434565495619834253255337377215694753592286	1.53×10^{74}
42	216986756631083658126920483628112951666071397627189154421561640107221284432844801035428489	2.16×10^{89}
49	310088432970902850840181144241298501449250543248054859810901973445648309893435820168570918245049037410431	3.10×10^{104}
56	445892162864331607261451155459356075903267153098914431766555207582747419210216766637190399627372668533451676732583464255	4.45×10^{119}
63	643721881546841017370450038311965896835937184278318037273509635473564403389071736713287672464233401686402393603351620144328030764295861	6.43×10^{134}
70	931801653317154380405796079127491163178848775602726300987100894320086644389085463600516139586911636316099665808988346144688141670996126976005161734564	9.31×10^{149}
77	135130717548391423447584658711422595720339892692671913539703988794360732211891723708316848272305890430658156750009193142217895888685166422244704586802154247606947 1416	1.35×10^{165}
84	196228713200162411938978864181761876772101743989385885750500710865127833221308499197643973255639411782537399755819240889235207308904607213766931897164428188907008625400301874158061 1	1.96×10^{180}

Table 2: The number of fine triangulations of the right lattice triangle defined by the vertices $(0,0),(7,0)$, and $(0,n)$ for $n = 7, 14, \ldots, 84$. Note that $T_{7,84}$ corresponds to f_{10}.

3 Lower Bounds

Equation (2.6) provides an improved upper bound on the count of diffeomorphism classes of CYs. In lieu of an answer to the complementary question of finding a lower bound on the number of such diffeomorphism classes, we work towards answering a related, pragmatic question: that of finding a lower bound on the number of 2-face equivalence classes. For two triangulations to define non-diffeomorphic CYs, they must have different 2-face restrictions and hence lie in different classes. However, this count fails to be a lower bound on the count of diffeomorphism classes because the converse need not hold: as in [2, 3], distinct 2-face equivalence classes may lie in the same diffeomorphism class.

No methods are currently known for efficiently checking diffeomorphism at arbitrary $h^{1,1}$ as, most directly, this would require determining if an integral $h^{1,1} \times h^{1,1}$ change of basis matrix exists relating the intersection numbers and second Chern class. Therefore,

2-face	Old Bound (from [1])	Type	New Bound	Type
f_8	411376139330301510538742295639337626245683966408394965837152256 ($\sim 4.11 \times 10^{62}$)	Upper FT	2021150258263610784069264594661003440 ($\sim 2.02 \times 10^{35}$)	Exact FRT
f_9	17498005798264095394980017816940970922825355447145699491406164851279623993595007385788105416184430592 ($\sim 1.75 \times 10^{100}$)	Upper FT	76134298294428934909961850722820007848128150060091275780156805977 5 ($\sim 7.61 \times 10^{65}$)	Exact FT
f_{10}	57277807836949922408837567867349676981443478344341305058888289940462212801070580831869056853164925675085871901843799944014879372151414675340089005208312915924102574861595842420453360252295795755249008001646349049495186110721347516723071757421294859592 ($\sim 5.73 \times 10^{250}$)	Upper FT	19622871320016241193897886418176187677210174398938588575050071086512783322130849919764397325563941178253739975581924088923520730890460721376693189716442818890700862540030187415806 11 ($\sim 1.96 \times 10^{180}$)	Exact FT

Table 3: Upper bounds of FRTs of the three remaining 2-faces of our polytope. These constitute our main results on upper bounds.

typically, representatives from 2-face equivalence classes (commonly called 'NTFEs' for non-two-face-equivalent triangulations) are treated as a sufficiently irredundant set of CYs. Moreover, [14] demonstrates how to iterate directly over 2-face equivalence classes efficiently, and so the number of such classes is proportional to the current computational expense of iterating over all potentially-distinct CYs.

To then bound the number of 2-face equivalence classes from below, one must understand which collections of triangulations $\{\mathcal{T}_1, \ldots, \mathcal{T}_N\}$ of 2-faces $\{f_1, \ldots, f_N\}$ correspond to a 2-face equivalence class. For a 2-face equivalence class to exist, there must be some FRST of Δ° which, upon restriction to each f_i, generates the imposed triangulation $\mathcal{T}_i$. A necessary condition is that each $\mathcal{T}_i$ be fine and regular on f_i. However, this is not sufficient – collections of fine, regular 2-face triangulations exist which do not admit an FRST of Δ°. This is the notion of 'extendability' from [14]. Thus, our goal is to bound from below the number of collections of 2-face triangulations for which such an FRST of Δ° provably exists.

To understand how extendability can fail, consider a similar problem of 'patching' together two 2D lattice triangulations[10]. For notation, let $P_{m,n} := \{0, 1, \ldots, m\} \times \{0, 1, \ldots, n\}$ be the $m \times n$ lattice rectangle. While any fine triangulation of P_{m,n_1} and any other fine triangulation of P_{m,n_2} can be patched together to form a fine triangulation of P_{m,n_1+n_2}, the same cannot be said of fine *regular* triangulations. In particular, see Figure 4 for an example of two fine, regular triangulations that, when 'patched', lead to an irregular triangulation.

[10] Although, we stress, this slightly varies from the extendability issue.

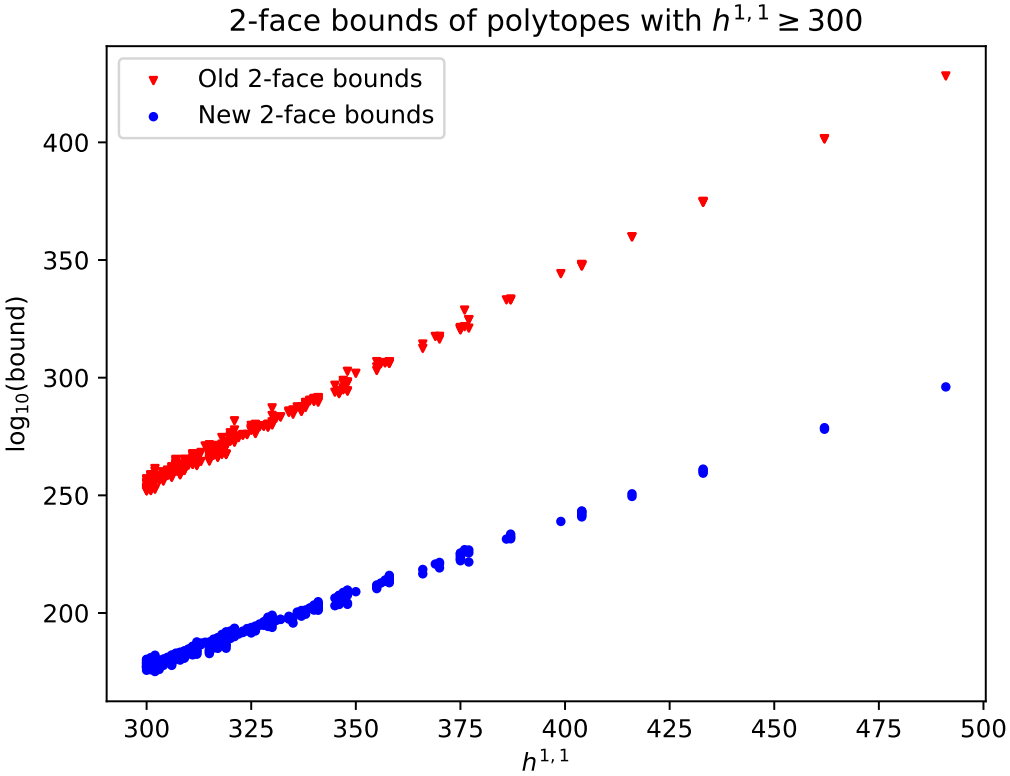

Figure 3: Improvements in the upper bounds on the number of 2-face equivalence classes for polytopes with $h^{1,1} \geq 300$, comparing those computed in [1] (red) with those found in this work (blue).

This failure mirrors that of extendability: in both cases, despite starting with regular triangulations, there may not be any height vector defining the combined object. There will be some instances in which regularity *can* be preserved via patching which will be discussed in the next subsection.

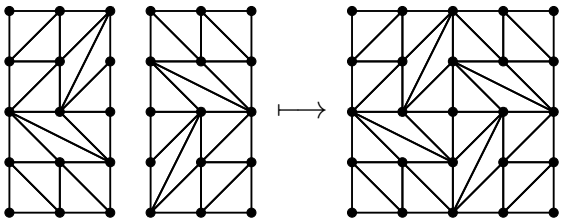

Figure 4: Two fine regular triangulations of $P_{2,4}$ being patched to a single triangulation of $P_{4,4}$. This triangulation is fine but not regular. This example was originally found by Francisco Santos and appears in [20].

3.1 Lower bounds for Δ°_{491}

In light of extendability, to generate a lower bound on the number of 2-face equivalence classes, we must generate *compatible* collections of fine, regular 2-face triangulations. Given that the upper bound on Δ°_{491} dominates, we focus our subsequent analysis to

this particular polytope. Specifically, we do so by first generating a lower bound on the number of fine, regular triangulations of the largest 2-face f_{10}. From this 2-face, we then lower-bound the number of compatible fine, regular triangulations of the remaining 2-faces, i.e. those which, together with the triangulation of f_{10}, are provably extendable to an FRST of Δ°_{491}.

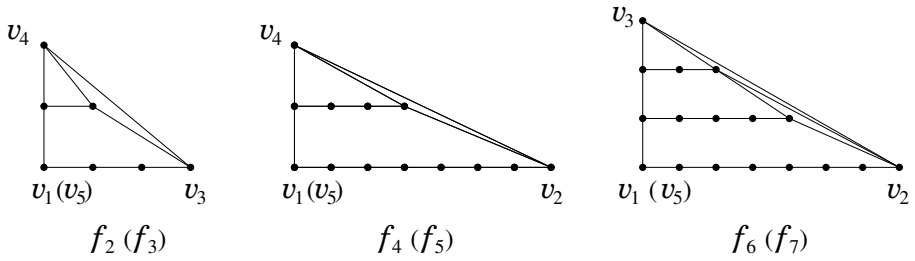

Figure 5: The primary subdivisions of $f_2, \ldots, f_7$. Primary subdivisions of f_8 and f_9 are described in the text. The vertices $v_1, \ldots, v_5$ of Δ°_{491} are numbered as the columns of (1.2).

As will be shown in Section 3.2, any fine regular triangulation of f_{10} is compatible with maximal refinements of what we call the *primary subdivisions* of the other 2-faces. For the primary subdivisions of $f_2, \ldots, f_7$, see[11] Figure 5. Recall from Table 1 that f_8 is a right triangle of width 2 and height 84; the primary subdivision of f_8 is splitting the 2-face into two width 1 strips. Similarly, f_9 is a right triangle of width 3 and height 84; the primary subdivision is splitting the 2-face into three width 1 strips.

We need to both bound, from below, $N_{\mathrm{FRT}}(f_{10})$, as well as count the number of maximal refinements of the primary subdivisions. First, some technology which motivates the primary subdivisions.

Lemma 3.1 (Proposition 3.4 in [20])**.** *For $n \geq 1$, the following hold:*

$$N_{\mathrm{FRT}}(P_{1,n}) = N_{\mathrm{FT}}(P_{1,n}) = \binom{2n}{n},$$
$$N_{\mathrm{FRT}}(P_{2,n}) = N_{\mathrm{FT}}(P_{2,n}).$$

Lemma 3.1 tells us that any fine triangulation of a width 1 or width 2 lattice rectangle is regular. We use this extensively with the following lemma, which shows that one can add strips of width 1 to a regular triangulation without spoiling the regularity.

Lemma 3.2 (Lemma 3.5 in [20][12])**.** *For $m, n \geq 1$, the following holds:*

$$N_{\mathrm{FRT}}(P_{m+1,n}) \geq N_{\mathrm{FRT}}(P_{m,n}) \cdot \binom{2n}{n}.$$

Lemma 3.2 can be understood as: given a regular triangulation of $P_{m,n}$, we may append any triangulated width 1 strip and maintain regularity of $P_{m+1,n}$. Alternatively, a deconstructive viewpoint may be taken, where we decompose $P_{m,n}$ entirely into width 1 strips, obtaining the lower bound $N_{\mathrm{FRT}}(P_{m,n}) \geq \binom{2n}{n}^m$. This decomposition mirrors our primary subdivisions. Applying the second line of Lemma 3.1, one may slightly improve

[11] f_1 is trivial because it has one triangulation: it is the unit simplex.

[12] As stated, there is a typo in Lemma 3.5 in [20]. This is however an easy fix: the binomial coefficient is $\binom{2m}{m}$ rather than $\binom{2n}{n}$. The general argument provided still holds true.

this bound by decomposing until there is exactly one width 2 strip and a collection of width 1 strips.

Lemmas 3.1 and 3.2 were proven via a more general lemma regarding regularity of lattice trapezoids of width 1. Note that lattice trapezoids of width 1 with parallel sides of lattice lengths m and n follow a similar formula to Lemma 3.1: the number of fine regular triangulations is $\binom{n+m}{n}$. The upshot of using lattice trapezoids rather than lattice rectangles is that the arguments used in Lemmas 3.1 and 3.2 directly generalize to the lattice polygons in Figure 5.

Lemma 3.3 (Lemma 3.3 in [20]). *Let $\mathcal{T}$ be a fine triangulation of a lattice trapezoid with two parallel vertical or horizontal sides S_0 and S_1 at distance one. Every piecewise linear function $h_0 : S_0 \to \mathbb{R}$ that is strictly convex on $S_0 \cap \mathbb{Z}^2$ can be extended to a lifting function for $\mathcal{T}$.*

This lemma provides significant freedom in the choice of lifting function/height vector; for instance, given a lifting function produced by Lemma 3.3 above, one can produce another lifting function by raising the entire side S_1 by a constant height, effectively fixing the height of any single point on S_1. We will use this extensively in Section 3.2. Altogether, these lemmas now guarantee that any fine triangulation refining the primary subdivision of each f_i is also regular. Using the preceding lemmas, we can now count the number of such refinements.

All that remains is to compute a lower bound on $N_{\mathrm{FRT}}(f_{10})$. Recall from Table 1 that f_{10} is a right triangle of width 7 and height 84. We compute a lower bound by decomposing the 2-face into one strip of width 2 and five strips of width 1. Varying the placement of the strip of width 2 and using inclusion-exclusion then gives a lower bound:

$$\begin{aligned} N_{\mathrm{FRT}}(f_{10}) \geq\ & 61629753637666384249294886276486436545694516976935412544055123 \\ & 51854904014562566277633806026740716703726964245039569074175193995 \\ & 63432314021032777216390798881136475500000 \\ & \approx 6.16 \cdot 10^{167}. \end{aligned} \tag{3.1}$$

One can compute this directly from binomial coefficients and (A.2).

We claim that any fine regular triangulation of f_{10} and any collection of maximal refinements of the primary subdivisions of $f_2, \ldots, f_9$ extends to a fine regular star triangulation of Δ°_{491}. We show this below in Section 3.2. This implies

$$\begin{aligned} N_{\mathrm{FRST}}(\Delta^\circ_{491}) \geq\ & N_{\mathrm{FRT}}(f_{10}) \cdot \binom{140}{56}\binom{84}{28} \cdot \binom{126}{42} && \text{[contribution of } f_{10},\ f_9,\ f_8\text{]} \\ & \times \binom{11}{4}^2 \binom{6}{2}^2 \cdot \binom{10}{3}^2 \cdot \binom{4}{1}^2 && \text{[contribution of } f_7, \ldots, f_2\text{]} \\ \geq\ & 15481007102006939736194364533953509004122317171981255190656 \\ & 33110923739140266773147074375773477934173844184524742007938 11 \\ & 60336678937504067409541550939890363008023562170734011537938 35 \\ & 53011884181791238182664073835437653215594056096511774595973 94 \\ & 60369630358603308800000000000000000 \\ & \approx 1.55 \cdot 10^{276}, \end{aligned} \tag{3.2}$$

where we apply the lower bound (3.1) found above. See Table 4 to compare individual

2-face contributions to either the total number of FRTs of the 2-face (or an upper bound of this quantity); this gives a sense as to how tight the bounds are on individual 2-faces.

One can look to increase the lower bound by improving the lower bound of $N_{\mathrm{FRT}}(f_{10})$. One way to do this would be to take into account contributions of larger-width trapezoids; this is explored in Appendix D. However, we gain a factor of less than 10 and so omit this from the main text, instead using the bound (3.1) above.

3.2 Proof of extendability

Here, we argue that any collection of maximal refinements of the primary subdivisions of the 2-faces is extendable (i.e., there exists an FRST with said restrictions). Let $v_1, \ldots, v_5$ be the vertices of Δ°_{491} numbered as the columns of (1.2). Then, the 2-faces are

$$\begin{gathered} f_1 = [v_2, v_3, v_4], \\ f_2 = [v_1, v_3, v_4], \quad f_3 = [v_5, v_3, v_4], \\ f_4 = [v_1, v_2, v_4], \quad f_5 = [v_5, v_2, v_4], \\ f_6 = [v_1, v_2, v_3], \quad f_7 = [v_5, v_2, v_3], \\ f_8 = [v_1, v_4, v_5], \quad f_9 = [v_1, v_3, v_5], \quad f_{10} = [v_1, v_2, v_5], \end{gathered}$$

and the edges have lattice lengths

$$\begin{gathered} |v_1v_5| = 84, \quad |v_1v_2| = |v_2v_5| = 7, \quad |v_1v_3| = |v_3v_5| = 3, \quad |v_1v_4| = |v_4v_5| = 2, \\ |v_2v_3| = |v_2v_4| = |v_3v_4| = 1. \end{gathered}$$

2-face	Contribution to the lower bound (3.2)	Upper bound of N_{FRT}
f_1	1	1*
f_2, f_3	4	5*
f_4, f_5	120	204*
f_6, f_7	4950	19594*
f_8	5.09×10^{33}	2.02×10^{35}*
f_9	8.73×10^{61}	7.61×10^{65}
f_{10}	6.16×10^{167}	1.96×10^{180}

Table 4: Contributions to the lower bound (3.2) by 2-face. In the right-most column, we also list the total number N_{FT}, or, if known, the total number N_{FRT} of the 2-face. Starred quantities denote exact counts of FRTs.

Fix an arbitrary collection of triangulations refining the primary subdivisions of f_i. We show that there exists an FRST of Δ°_{491} which restricts to this collection of 2-face triangulations. In order to prove this fact, we construct a piecewise linear function h (the height function) on the boundary of Δ°_{491} such that the restriction of h to each 2-face f_i refines the primary subdivisions to the chosen triangulations. We do so by defining height functions h_i on every 2-face which refine the primary subdivisions to triangulations, and which are compatible with one another.

We give a brief overview of the construction of h_i: first, we define functions g_i on each 2-face such that lifting face f_i by g_i gives precisely the primary subdivision (not a proper refinement of it). Next, we define functions k_i on each 2-face such that the restriction of k_i to any *cell* of the primary subdivision of f_i agrees with the triangulation on this cell; note

that lifting the entire 2-face f_i by k_i need not give the chosen triangulation of f_i. However, when adding k_i to a sufficiently large multiple of g_i, then k_i acts as a perturbation of g_i, and lifting f_i by this sum gives our triangulation. Note that care still must be taken in the construction to ensure compatibility between 2-faces, as we see below.

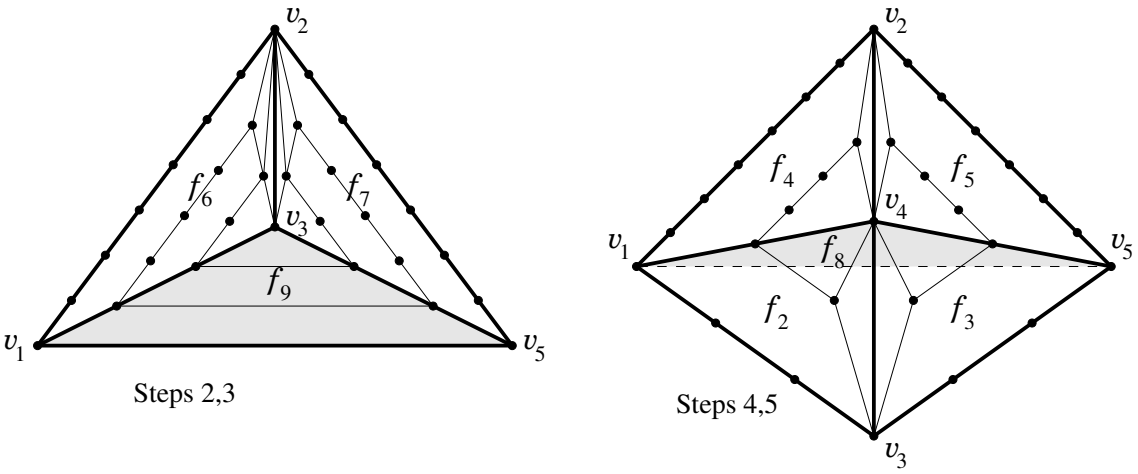

Figure 6: Left: a diagram of the 3-face 1235 of Δ°_{491}. The face f_{10} is obscured. Dots indicate lattice points, except for f_9 which has 172 lattice points, so we just shade it gray. The displayed lines indicate the primary subdivisions, as in Figure 5. Right: an analogous diagram showing details of the rest of polytope Δ°_{491}, now with the 3-face 1235 as the base. The remaining faces with v_4 as a vertex are visible. Face f_8 cuts through the figure and is represented by the shaded region above the dashed line.

The construction of h goes as follows (see Figure 6).

Step 1. By hypothesis we may define such an h on f_{10}. By Lemma 3.3 the restriction of h to the edge $[v_1, v_5]$ can be extended (strip by strip) to piecewise linear functions k_8, k_9 on f_8, f_9 such that on any cell of the respective 2-face, k_8 and k_9 refine the cell to the imposed triangulation.

Step 2. Using Lemma 3.3 we extend (strip by strip) the restriction $h|_{[v_1,v_2]}$ from f_{10} to a piecewise linear function k_6 on $f_6 = [v_1, v_2, v_3]$ so that k_6 is compatible with the chosen imposed triangulation of each cell of the primary subdivision and so that the restriction of k_6 to the edge $[v_1, v_3]$ coincides with k_9. We may impose this latter restriction because of the freedom afforded to us by the lemma. We also extend $h|_{[v_5,v_2]}$ to a function k_7 on $f_7 = [v_5, v_2, v_3]$ in the same way, in particular, so that $k_7|_{[v_5,v_3]} = k_9|_{[v_5,v_3]}$.

Step 3. Let g_6, g_7, g_9 be piecewise linear functions on f_6, f_7, f_9 compatible with the primary subdivisions and such that

1. $g_6|_{[v_1,v_3]} = g_9|_{[v_1,v_3]}$,
2. $g_7|_{[v_5,v_3]} = g_9|_{[v_5,v_3]}$, and
3. $g_6|_{[v_1,v_2]} = g_7|_{[v_5,v_2]} = g_9|_{[v_1,v_5]} = 0$.

Then we define $h_i = k_i + Ag_i$ on the 2-faces f_i, $i = 6, 7, 9$ for $A \gg 1$. This now ensures that the various h_i generate the desired triangulations on f_i, and that the h_i are compatible on their shared faces. We now define h on f_i, $i = 6, 7, 9$ to be h_i. Therefore, we have defined h on the boundary of the 3-face $[v_1, v_2, v_3, v_5]$.

Step 4. (Similar to Step 2.) Using Lemma 3.3 we extend h as follows:

1. from $[v_1, v_3]$ to k_2 on $f_2 = [v_1, v_3, v_4]$,
2. from $[v_5, v_3]$ to k_3 on $f_3 = [v_5, v_3, v_4]$,
3. from $[v_1, v_2]$ to k_4 on $f_4 = [v_1, v_2, v_4]$, and
4. from $[v_5, v_2]$ to k_5 on $f_5 = [v_5, v_2, v_4]$.

As above, we perform these extensions so that the resulting functions $k_2, \ldots, k_5$ are piecewise linear, compatible with the triangulations of the cells of the primary subdivisions, and so that $k_2|_{[v_1,v_4]} = k_4|_{[v_1,v_4]} = k_8|_{[v_1,v_4]}$ and $k_3|_{[v_5,v_4]} = k_5|_{[v_5,v_4]} = k_8|_{[v_5,v_4]}$.

Step 5. (Similar to Step 3.) Let $g_2, \ldots, g_5$, and g_8 be the piecewise linear functions on $f_2, \ldots, f_5$ which are compatible with the primary subdivisions, vanish on the edges where h is already defined (i.e. on the edges of the 3-face $[v_1, v_2, v_3, v_5]$), and coincide on the common edges; thus these functions take the same value at v_4 and they take the same value at the midpoints of the segments $[v_1, v_4]$ and $[v_5, v_4]$. We define h_i on f_i, $i = 2, 3, 4, 5, 8$, to be $h_i = k_i + Bg_i$ with $B \gg A$.

Step 6. Finally, we define h on 2-faces f_i, $i = 2, 3, 4, 5, 8$ to be h_i. We extend h to f_1 by linearity. We further impose that the height of the origin is sufficiently small such that h also defines a star triangulation. Now, the constructed h defines the FRST of interest.

4 Conclusion

In this work, we have demonstrated that Batyrev's construction applied to FRSTs of 4D reflexive polytopes defines at most 10^{296} diffeomorphism classes of Calabi-Yau threefolds, improving [1]'s bound of 10^{428}. Both bounds arise by bounding the number of 2-face equivalence classes as in (2.1) – the only difference is that for 2-faces with more than 17 lattice points, we used the exact number of fine triangulations while [1] used Anclin's upper bound on the number of fine triangulations.

Specifically, we studied the number of 2-face equivalence classes for polytopes with $h^{1,1} \geq 300$. We studied only polytopes with $h^{1,1} \geq 300$ since the pre-existing bounds from [1] depend roughly exponentially on $h^{1,1}$, with all $h^{1,1} < 300$ polytopes contributing only 10^{259} to the bound. We find that this exponential dependence is still true after our improvement (see Figure 3); namely, our final bound is still ultimately set by the largest-$h^{1,1}$ polytope, Δ°_{491}. Indeed, we show that the polytopes with $300 \leq h^{1,1} < 491$ contribute 10^{279} to the upper bound, orders-of-magnitude smaller than Δ°_{491}'s contribution of 10^{296}.

In addition to the above results on upper bounds of the number of 2-face equivalence classes, we demonstrated a lower bound of 10^{276} such classes for Δ°_{491}. This was obtained by defining 'primary subdivisions' of the faces $f_1, \ldots, f_9$, analogous to the decompositions utilized in [20], and proving that, for any FRT of f_{10} and any maximal refinement of said subdivisions, there exists an FRST of Δ°_{491} with said 2-face restrictions. That is, these 2-face triangulations are extendable. Thus, our upper bound of 10^{296} 2-face equivalence classes is loose by at most 20 orders of magnitude. Of particular interest for this upper bound are f_9 and f_{10}, for which we utilized counts N_{FT} in (2.1). If one instead had exact counts N_{FRT} for these faces, this upper bound could drop by at most 17 orders of magnitude (see Table 4).

The state-of-the-art in generating potentially-inequivalent CYs is by constructing representatives of each 2-face equivalence class as in [14]. Thus, using current methods,

studies of all Kreuzer-Skarke CYs with $h^{1,1} = 491$ must operate on at *least* 10^{276} CYs. It is computationally infeasible to study 10^{276} CYs – even if such a hypothetical study took 1 femptosecond per CY, it would still take at least 10^{261} seconds to study all of them. For such a study to be viable, one would need an algorithm to directly construct (not stepping through, e.g., 2-face equivalence classes) an exponentially smaller collection of all potentially non-diffeomorphic CYs, should it exist.

One natural direction for future study is to adapt these bounds in light of the generalizations to the construction of CYs from 4D reflexive polytopes discussed in [11, 12]. Currently, this is non-trivial as it requires defining a clean notion of 2-face equivalence for such CYs. Another direction would be to better determine the true distribution of inequivalent CYs. A first step towards this goal would be to obtain a non-trivial lower bound on the number of diffeomorphism classes of CYs, as opposed to the lower bound on 2-face equivalence classes found in this work. To the best of the authors' knowledge, such a non-trivial lower bound on diffeomorphism classes is not known; moreover, despite Δ°_{491} having at least 10^{276} 2-face equivalence classes, it has not been demonstrated that these define at least two non-diffeomorphic CYs. One approach could be coming up with novel invariants of the Wall data; while we can compute the triple intersection numbers and second Chern class, it is hard to determine whether or not there exists a change of basis between these data. On the other hand, the invariants in [2, 3] (such as the GCD invariants) are easy to work with but have low discriminative power and are hence well-suited only to low-$h^{1,1}$ CYs. Searching for more powerful but still computationally practical invariants is a worthwhile endeavor.

Acknowledgments

NM and MS are grateful to Volker Kaibel, Liam McAllister, Andres Rios-Tascon, and Francisco Santos for helpful correspondence. MS would also like to thank Pyry Kuusela for providing valuable feedback on an earlier version of the draft. The work of NM and MS is supported in part by NSF grant PHY-2309456.

A Right lattice trapezoids of width 2

As discussed in Section 2, for the largest 2-faces f_8, f_9, and f_{10} of Δ°_{491}, we use a recursive algorithm of [21] to compute the exact count of fine triangulations. However, following [20], we also introduce a recursive algorithm designed specifically to tackle right lattice trapezoids of width 2, including the third-largest 2-face f_8. This algorithm additionally can be used when computing the bound (3.1).

First setting notation following [20, 21], define

$$f(m,n) \coloneqq N_{\mathrm{FT}}(P_{m,n}) \qquad \text{and} \qquad f^{\mathrm{reg}}(m,n) \coloneqq N_{\mathrm{FRT}}(P_{m,n}). \tag{A.1}$$

Section 2.1 of [20] discusses determining the exact count of fine triangulations of narrow lattice strips via a recursive algorithm. For lattice trapezoids of width $m = 1$, with parallel sides of lattice lengths a and b, the number of fine triangulations is exactly $g_1(a,b) \coloneqq \binom{a+b}{a} = \binom{a+b}{b}$.

For strips of width $m = 2$ and arbitrary height n, [20] makes the observation that to count all fine triangulations, one can enumerate the triangulations by their highest *width 2 diagonal*, where a width 2 diagonal is an internal edge of horizontal length two but

lattice length 1 (i.e., its midpoint is not a lattice point). This diagonal then decomposes the width 2 strip into two 'non-interacting' width 1 strips which lie above the diagonal, as well as the trapezoid determined by the diagonal. See Figure 7 below.

This observation still holds when considering *right-lattice trapezoids* of width $m = 2$. We consider those whose upper boundary has integral slope (which describes e.g. f_8 and the width 2 strips used in Section 3.1's bound of $N_{\text{FRT}}(f_{10})$), but note that this can be further generalized. Let our lattice trapezoid be determined by $\text{conv}\{(0,0),(0,n),(2,0),(2,n+2k)\}$ where k is a non-negative integer. In analog with (A.1), let $f(2;n,k)$ (resp. $f^{\text{reg}}(2;n,k)$) denote the number of fine (resp. fine regular) triangulations of this trapezoid.

Then, to count all fine triangulations, we count the number of fine triangulations for each configuration determined by a placement of the highest width 2 diagonal $\overline{AB}$. This can be split into two terms: (1) the lack of a placement of a diagonal, and (2) a valid placement of the upper diagonal $\overline{AB}$, where A lies on the left boundary of the trapezoid and B on the right boundary. Term (1) can be computed as the product of the number of fine triangulations of the non-interacting width 1 strips. Each summand in term (2), determined by $\overline{AB}$, can be computed as the product of the number of fine triangulations of the non-interacting strips above the diagonal and the number of fine triangulations of the trapezoid $\text{conv}\{(0,0),(0,A),(2,0),(2,B)\}$. Again, see Figure 7 below for this decomposition. Let $g_2(A,B)$ be the number of fine triangulations of this trapezoid, where the explicit recursion for $g_2(A,B)$ can be found in [20]. Then:

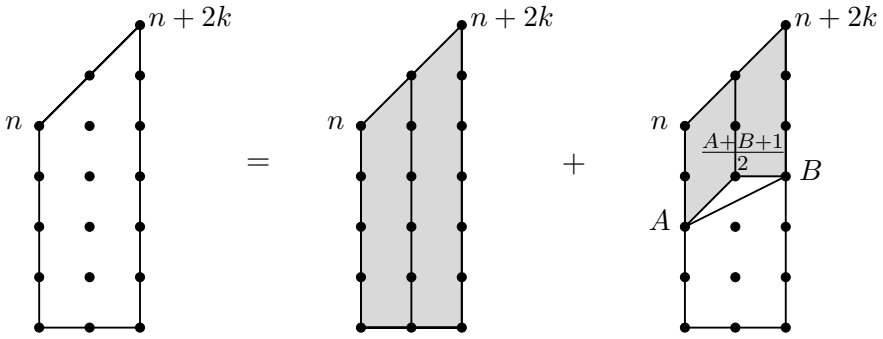

Figure 7: The deconstruction of fine lattice triangulations into two non-interacting width 1 strips and a sum over triangulations determined by the highest width 2 diagonal $\overline{AB}$. The sum over diagonals is left implicit.

$$f(2;n,k) = \binom{2n+k}{n}\binom{2n+3k}{n+2k} + \sum_{\substack{0\le A\le n \\ 0\le B\le n+2k \\ A+B\equiv 1 \,(\text{mod } 2)}} g_2(A,B)\binom{2n+k-\frac{3A+B+1}{2}}{n-A}\binom{2n+3k-\frac{A+3B+1}{2}}{n+2k-B}. \tag{A.2}$$

As this lattice trapezoid is width 2, we note that as in Lemma 3.1:

$$f^{\text{reg}}(2;n,k) = f(2;n,k). \tag{A.3}$$

Therefore, we have a recursive algorithm which can be used to find the exact number of fine, regular triangulations of right lattice trapezoids whose upper boundary is integral. Extending this style of formula beyond width 2 lattice trapezoids above can be done, but will be less efficient than the method described in detail in Appendix B.

B Counting fine triangulation of rectangles of a fixed width

The improvement [21] of the dynamic programming algorithm from [20] is as follows.

An *admissible shape* S of width m is a lattice polygon which is cut from the strip $[0,m]\times[0,+\infty]$ by the graph of a non-negative continuous piecewise-linear function ϕ, i.e.,

$$S=\{(x,y)\mid 0\le x\le m,\ 0\le y\le\phi(x)\}.$$

We say that a lattice polygon Q is a *primitive tile* in the following three cases:

1. Q is a primitive lattice triangle without vertical sides;
2. Q is a primitive lattice triangle whose vertical side is contained in the boundary of the strip $0\le x\le m$;
3. $Q=\Delta_1\cup\Delta_2$ where Δ_1 and Δ_2 are primitive lattice triangles such that $\Delta_1\cap\Delta_2$ is a common vertical side of Δ_1 and Δ_2.

A primitive tile Q is *S-maximal* for an admissible shape S if $Q\subset S$ and the upper part of the boundary of Q is contained in the upper part of the boundary of S, i.e.,

$$\max_{(x,y)\in Q} y=\max_{(x,y)\in S} y$$

for any x such that $Q\cap(\{x\}\times\mathbb{R})$ is non-empty.

We say that S' is an *admissible subshape* of an admissible shape S and we write $S'\prec S$ if S' is the closure of $S\setminus(Q_1\cup\dots\cup Q_k)$, $k\ge 1$, where $Q_1,\dots,Q_k$ are S-maximal primitive tiles with pairwise disjoint interiors. In this case we set $\#(S',S)=k$. Note that the relation "to be an admissible subshape" is not transitive.

Denote the number of primitive triangulations of an admissible shape S by $f(S)$. The following lemma is the inclusion-exclusion formula in our setting (see [21, Lemma 2.2]; cf. [20, Lemma 2.2]).

Lemma B.1. *For any admissible shape S we have (see Figure 8)*

$$f(S)=\sum_{S'\prec S}(-1)^{\#(S',S)-1}f(S'). \tag{B.1}$$

This gives us the following dynamic programming algorithm for computation of $f(S)$ for a given shape S of width m. We start by setting $f(S)=1$ for $S=[0,m]$ (the shape with the empty interior). Then, successively for $A=1,2,\dots,2mn$, we compute $f(S)$ for all shapes (included in $P_{m,n}$) of area A by formula (B.1), using the previously computed shapes of smaller areas (here we normalize the area so that the area of primitive lattice triangles is 1). The area of a shape with the upper boundary $[(x_0,y_0),(x_1,y_1),\dots,(x_k,y_k)]$ ($x_0=0$, $x_k=m$) is equal to

$$\sum_{i=0}^{k} s_i y_i,\qquad \text{where } s_i=(x_{i+1}-x_{i-1}) \text{ and } x_{-1}=0,\ x_{k+1}=m. \tag{B.2}$$

The following is a `Wolfram Mathematica` code that computes the number of primitive triangulations of the triangles $T_{3,3n}$, $n=1,\dots,28$ (recall that $f_9\cong T_{3,84}$). The computation takes $\sim$2 seconds.

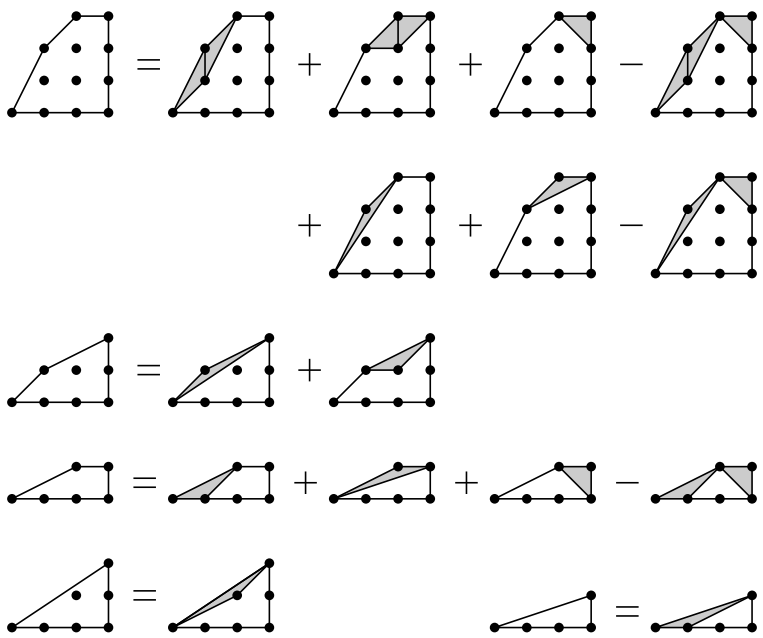

Figure 8: Inclusion-exclusion formula for admissible shapes.

```
F[0,0,0]=1;              (* F[b,c,d] = f( [(0,0),(1,b),(2,c),(3,d),(3,0)] ) *)
Do[                            (* G1[c,d] = f( [(0,0), (2,c),(3,d),(3,0)] ) *)
   Do[ d = area - 2*b - 2*c; (* G2[b,d] = f( [(0,0),(1,b), (3,d),(3,0)] ) *)
     If[ d<0 || d>84, Continue[], F[b,c,d]=0 ];
     If[ b>0, F[b,c,d] += F[b-1,c,d] ];  If[ c>0, F[b,c,d] += F[b,c-1,d] ];
     If[ d>0, F[b,c,d] += F[b,c,d-1]; If[ b>0, F[b,c,d] -= F[b-1,c,d-1] ] ];
     If[ 2*c==b+d+1, F[b,c,d] += G2[b,d] ];
     If[ 2*b==c+1, F[b,c,d] += G1[c,d]; If[ d>0, F[b,c,d] -= G1[c,d-1] ] ],
   {b,0,28},{c,0,56}];
   Do[ d = area - 3*c; b = (c-1)/2;
     If[ d<0 || d>84, Continue[], G1[c,d] = F[b,c,d] ];
     If[ d>0, G1[c,d] += (G1[c,d-1] - F[b,c,d-1]) ];
     If[ 3*c == 2*d + 1, G1[c,d] += G2[b,d] ],
   {c,1,55,2}];
   Do[ d = (area - 3*b)/2; c = (b+d-1)/2;
     If[ d<0 || d>84 || Mod[b+d,2]==0, Continue[], G2[b,d] = F[b,c,d] ];
     If[ 3*b == d + 1, G2[b,d] += G1[c,d] ],
   {b,Mod[area,2],28,2}];
   If[ Mod[area,9]==0, b=area/9; Print[F[b,2b,3b]] ],
{area,1,3*84}]
```

C Estimates of the complexity

Here we discuss the complexity of the above algorithm in the case of rectangles $P_{m,n} = [0,m] \times [0,n]$. The total number of admissible shapes is bounded above by $(n+2)^{m+1}$. Indeed, each shape $S \subset P_{m,n}$ can be encoded by a sequence $(y_0, \ldots, y_m)$, where $0 \le y_k \le m$ if (k, y_k) belongs to the upper boundary of S, and $y_k = n+1$ if the upper boundary does not contain an integral point on the vertical line $x = k$.

The arguments as in the proof of [20, Lemma 2.5] give a (rather coarse) upper bound $3 \cdot 2^{m-1}$ for the number of admissible subshapes of a given shape. Thus the total number of the additions in (B.1) during the whole computation is bounded by

$$3 \cdot 2^{m-1}(n+2)^{m+1}.$$

However, as it is pointed out in [20], "the bottleneck in the computations is always memory", and this is still so 20 years after. So, let us discuss the needed memory in more details.

When computing $f(S)$ for the shapes of a given area A, we need in fact to keep in the memory only the values of $f(S')$ for the shapes S' such that $A - m \le \mathrm{Area}(S') \le A$. Let us estimate the number of such shapes. It is convenient to do it in probabilistic terms. Let N_A be the number of shapes of area A. For a given subset $\xi = \{x_0, \dots, x_k\} \subset \{0, \dots, m\}$ such that $x_0 = 0$ and $x_k = m$, let $N_A(\xi)$ be the number of shapes S of area A contained in $P_{m,n}$ such that the integral points on the upper boundary of S are (x_i, y_i) for some integers $y_0, \dots, y_k$. Let $s_0, \dots, s_k$ be as in (B.2). Then we have

$$N_A(\xi) = \#\Big\{(y_0, \dots, y_k) \in \mathbb{Z}^{k+1} \;\Big|\; s_0 y_0 + \dots + s_k y_k = A,\ 0 \le y_i \le n\Big\}.$$

Let $X_0, \dots, X_k$ be independent random variables such that each X_i takes the values in $\{0, \dots, n\}$ with equal probabilities. Then $N_A(\xi) = (n+1)^{k+1}\mathbf{P}(s_0X_0 + \dots + s_kX_k = A)$. We have $s_0, s_k \ge 1$ and $s_i \ge 2$ if $0 < i < k$. Hence $s_0^2 \ge 2s_0 - 1$, $s_k^2 \ge 2s_k - 1$, and $s_i^2 \ge 2s_i$ if $0 < i < k$. We also have $\sum s_i = 2m$. Therefore:

$$s_0^2 + \dots + s_k^2 \ge 2(s_0 + \dots + s_k) - 2 = 4m - 2.$$

Since the variance of X_i is $((n+1)^2 - 1)/12$, by the Central Limit Theorem we have

$$N_A(\xi) \approx (n+1)^k \sqrt{\frac{12}{2\pi(s_0^2 + \dots + s_k^2)}} \le (n+1)^k \sqrt{\frac{3}{\pi(2m-1)}} < \frac{(n+1)^k}{\sqrt{2m-1}}$$

and then

$$N_A = \sum_k \sum_{|\xi|=k+1} N_A(\xi) \lesssim \sum_k \binom{m-1}{k-1} \frac{(n+1)^k}{\sqrt{2m-1}} < \frac{(n+2)^m}{\sqrt{2m-1}}.$$

Thus the number of the values of $f(S)$ that we need to keep simultaneously in the memory is bounded above by the quantity

$$\frac{N_{A-m} + \dots + N_A}{2} \lesssim \frac{(m+1)(n+2)^m}{2\sqrt{2m-1}} < \frac{(n+2)^m\sqrt{2m+7}}{4}$$

(the denominator 2 in the last formula comes from the symmetry of the rectangle $P_{m,n}$ with respect to the vertical axis).

By the same arguments we obtain that the maximal number of values of $f(S)$ that we need to keep in the memory during the computation of $f(T_{m,n})$ is

$$C_m n^m + O(n^{m-1}), \quad \text{where} \quad C_m = \frac{(m+1)!}{m^m\sqrt{2\pi\left(\frac{m^3}{9} - \frac{m^2}{12} + \frac{m}{18}\right)}} = \Big(3 + \tfrac{35}{8m} + O(m^{-2})\Big)e^{-m}.$$

D Further possible improvements to the lower bound of $N_{\mathrm{FRT}}(f_{10})$

There are further possible improvements that one can make to the lower bound of $N_{\mathrm{FRT}}(f_{10})$. One can recursively construct FRTs by the following distinct operations. Given FRTs of some trapezoids T, T_1, T_2, we can obtain an FRT of the larger trapezoids as shown in

Figure 9, where the common edge of T_1 and T_2 has lattice length 1. The width 1 patterns should be chosen so that the triangles in Figure 9 are minimal possible (in particular each of the triangle should be replaced by a segment if possible). It is not difficult to compute recursively the number of all FRTs of f_{10} that are obtained in this way.

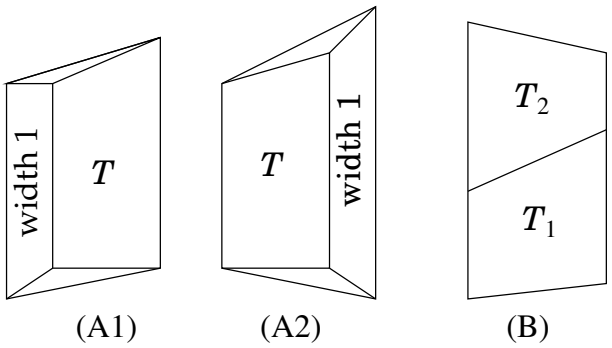

Figure 9: Recursive construction of FRTs. Any vertical side of T (and even both of them) may have zero length, i.e. T may be degenerated to a triangle or a segment. One of the vertical sides (but not both) of T_i also may have zero length.

This construction can be generalized by allowing the common edge of T_1 and T_2 (see Figure 9) to have lattice length 1 or 2. In this case the computation becomes more complicated because we have to exclude repeated counting of some FRTs; see Figure 10.

Some other improvements of this kind are also possible. For example, one can generalize the operations in Figure 9(B) to pentagons and hexagons, but the control of repeated counting becomes more and more complicated with less and less gain. The cumulative effect of all the improvements discussed in this section is an increase in the lower bound by a factor of less than 10. We thus do not explain them in detail.

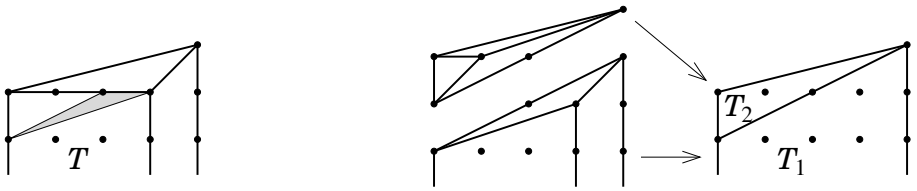

Figure 10: Precaution when the common edges in the operation (B) are allowed to have lattice length 2. If T is involved in the operation (A2) and its triangulation contains the gray triangle, then this triangulation can be also obtained by the operation (B), where the triangle T_2 is obtained by the operation (A1) from a segment (considered a trapezoid whose both vertical sides have zero length).

E Triangulation data for all relevant 2-faces

We first give in Table 5 a list of the 2-faces $\{f\}$ (up to affine equivalence) appearing in Kreuzer-Skarke polytopes with $h^{1,1} \geq 300$ as well as their associated fine triangulation counts $N_{\mathrm{FT}}(f)$. The list of 2-faces is indexed by: (1) area, from least to greatest, (2) number of edges, from least to greatest, and (3) edge lengths, treated lexicographically. In addition to an index, we present a list of vertices defining the 2-face, and note which polytopes the 2-face appears in. The 401 polytopes with $h^{1,1} \geq 300$ are 1-indexed, and are

presented in order of increasing $h^{1,1}$. For polytopes with the same $h^{1,1}$, they are ordered in the same manner as is found on a webpage maintained by Skarke [24]. We then denote the multiplicity of a given 2-face appearing in a polytope by an exponent.

Table 6 then follows the indexing in Table 5 and provides an exact count of $N_{\mathrm{FT}}(f)$. We note that for all 2-faces with at most 17 lattice points in this list, $N_{\mathrm{FT}}(f) = N_{\mathrm{FRT}}(f)$, except for the 2-faces 70, 76, and 77, which have $N_{\mathrm{FRT}}(f)$ equal to 14295, 19594, and 37085 respectively. These data (along with those computed in [1]) can then be used to reproduce the upper bounds (2.3) and (2.4). They can also be downloaded from [25].

As described in Appendix B, the dynamical programming algorithm used in this paper to compute the number of fine triangulations for a lattice polygon also computes as intermediate data the number of fine triangulations of all admissible shapes (of the same width and with the same lower boundary) of the polygon. We note that while Appendix B talks about the special case in which the lower boundary is the horizontal segment $[0, m] \times \{0\}$, we may also allow the lower boundary to be the graph of a continuous piecewise-linear function ϕ_0 such that $\phi_0(x) \leq \phi(x)$ for all $x \in [0, m]$ (see [21, Section 2.1]). All of the 2-faces described below of width greater than three can be embedded in this more general way into one of the following 19 lattice polygons: $157, 185, 228, 237, 242, 244, 256, 287, 291, 293, 310, 314, 316, 323, 325, 328, 330, 332$ or 333. This style of computation was shown, for instance, in Table 2.

Table 5: 2-faces and their appearences in KS polytopes with $h^{1,1} \geq 300$.

Ind.	2-face Vertices	Polytope$^{\text{Multiplicity}}$
1	(0, 0), (0, 1), (1, 0)	1^4, 2^2, 3^3, 4^4, 5^4, 6^3, 7^3, 8^2, 9^4, 10^4, 11^3, 12^3, 13^4, 14^3, 15^3, 16^5, 17^7, 18^8, 19^{14}, 20^5, 21^4, 22^6, 23^3, 24^4, 25^1, 26^4, 27^6, 28^3, 29^5, 30^4, 31^2, 32^1, 33^4, 34^7, 35^{10}, 36^{15}, 37^6, 38^3, 39^4, 40^6, 41^7, 42^4, 43^4, 44^2, 45^5, 46^{14}, 47^{12}, 48^2, 49^5, 50^2, 51^6, 52^3, 53^2, 54^5, 55^5, 56^8, 57^2, 58^3, 59^6, 60^7, 61^7, 62^{12}, 63^1, 64^2, 65^2, 66^2, 67^3, 68^5, 69^2, 70^3, 71^5, 72^4, 73^8, 74^5, 75^6, 76^3, 77^2, 78^7, 79^2, 80^2, 81^5, 82^5, 83^4, 84^7, 85^4, 86^6, 87^8, 88^4, 89^1, 90^2, 91^6, 92^5, 93^8, 94^7, 95^{11}, 96^2, 97^4, 98^5, 99^3, 100^{11}, 101^{14}, 102^6, 103^7, 104^{10}, 105^2, 106^1, 107^1, 108^3, 109^3, 110^4, 111^2, 112^5, 113^5, 114^1, 115^2, 116^4, 117^{10}, 118^{11}, 119^{13}, 120^{11}, 121^8, 122^3, 123^3, 124^5, 125^2, 126^2, 127^4, 128^7, 129^{11}, 130^9, 131^{12}, 132^2, 133^2, 134^5, 135^5, 136^4, 137^7, 138^6, 139^9, 140^{13}, 141^2, 142^2, 143^5, 144^8, 145^{11}, 146^2, 147^9, 148^2, 149^2, 150^5, 151^3, 152^5, 153^3, 154^5, 155^2, 156^3, 157^6, 158^5, 159^6, 160^9, 161^4, 162^6, 163^{10}, 164^{12}, 165^3, 166^2, 167^2, 168^2, 169^3, 170^3, 171^5, 172^5, 173^3, 174^5, 175^5, 176^6, 177^5, 178^{12}, 179^2, 180^4, 181^2, 182^2, 183^2, 184^2, 185^5, 186^2, 187^3, 188^6, 189^7, 190^9, 191^7, 192^6, 193^2, 194^5, 195^6, 196^9, 197^{10}, 198^6, 199^1, 200^2, 201^1, 202^1, 203^1, 204^4, 205^2, 206^2, 207^2, 208^2, 209^4, 210^4, 211^2, 212^2, 213^2, 214^2, 215^{12}, 216^3, 217^1, 218^2, 219^1, 220^3, 221^1, 222^4, 223^3, 224^{12}, 225^{15}, 226^6, 227^1, 228^3, 229^2, 230^4, 231^4, 232^4, 233^4, 234^{11}, 235^{12}, 236^{14}, 237^4, 238^2, 239^2, 240^1, 241^4, 242^2, 244^1, 245^5, 246^2, 247^5, 248^8, 249^6, 250^5, 251^2, 252^9, 253^5, 254^3, 255^{11}, 256^2, 257^1, 258^4, 259^2, 260^2, 261^5, 262^2, 263^3, 264^6, 265^9, 266^{12}, 267^2, 268^5, 269^2, 270^3, 271^5, 272^3, 273^4, 274^4, 275^3, 276^2, 277^4, 278^3, 279^4, 280^3, 281^5, 282^6, 283^4, 284^4, 285^2, 286^1, 287^7, 288^2, 289^2, 290^5, 291^2, 292^2, 293^4, 294^1, 295^5, 296^{11}, 297^1, 298^4, 299^{10}, 300^{13}, 301^4, 302^9, 303^2, 304^2, 305^4, 306^2, 307^8, 308^2, 309^2, 310^5, 311^2, 312^3, 313^6, 314^2, 315^2, 316^2, 317^5, 318^3, 319^5, 320^3, 321^5, 322^2, 323^6, 324^1, 325^2, 326^1, 327^1, 328^4, 329^2, 330^2, 331^2, 332^4, 333^4, 334^2, 335^2, 336^4, 337^1, 338^3, 339^{12}, 340^6, 341^1, 342^4, 343^4, 344^4, 345^{11}, 346^{14}, 347^2, 348^2, 349^3, 350^9, 351^2, 352^2, 353^5, 354^3, 355^4, 356^4, 357^2, 358^4, 359^3, 360^5, 361^1, 362^{10}, 363^2, 364^2, 365^2, 366^5, 367^1, 368^2, 369^1, 370^1, 371^4, 372^2, 373^2, 374^4, 375^2, 376^1, 377^3, 378^1, 379^4, 380^{11}, 381^2, 382^4, 383^4, 384^2, 385^5, 386^2, 387^1, 388^2, 389^1, 390^4, 391^2, 392^4, 393^4, 394^2, 395^1, 396^2, 397^1, 398^4, 399^1, 400^4, 401^1

Ind.	2-face Vertices	Polytope$^{\text{Multiplicity}}$
2	(0, 0), (0, 2), (1, 0)	1^{5}, 2^{7}, 4^{1}, 5^{1}, 6^{2}, 7^{1}, 8^{5}, 9^{2}, 10^{2}, 11^{4}, 12^{3}, 13^{2}, 14^{5}, 15^{7}, 16^{5}, 17^{4}, 18^{5}, 19^{2}, 20^{6}, 21^{2}, 23^{1}, 24^{2}, 25^{3}, 26^{2}, 27^{1}, 28^{4}, 29^{6}, 30^{5}, 31^{6}, 32^{2}, 33^{1}, 34^{2}, 35^{1}, 36^{1}, 37^{5}, 38^{7}, 39^{6}, 41^{4}, 44^{4}, 45^{4}, 47^{4}, 48^{6}, 49^{5}, 50^{4}, 51^{5}, 52^{3}, 53^{3}, 54^{2}, 55^{5}, 56^{4}, 57^{3}, 58^{1}, 59^{1}, 60^{1}, 61^{4}, 62^{1}, 63^{1}, 64^{2}, 66^{2}, 67^{2}, 68^{2}, 69^{5}, 70^{4}, 71^{2}, 73^{2}, 74^{5}, 75^{5}, 76^{4}, 77^{8}, 78^{5}, 79^{3}, 80^{1}, 82^{2}, 83^{1}, 85^{4}, 86^{4}, 87^{3}, 88^{1}, 89^{2}, 90^{2}, 91^{2}, 92^{4}, 93^{3}, 94^{3}, 96^{4}, 97^{5}, 98^{3}, 99^{4}, 100^{1}, 102^{5}, 103^{5}, 104^{3}, 105^{3}, 106^{3}, 107^{1}, 108^{2}, 109^{1}, 110^{2}, 111^{3}, 112^{1}, 113^{1}, 114^{1}, 115^{2}, 116^{1}, 117^{1}, 118^{2}, 119^{1}, 121^{4}, 122^{7}, 123^{6}, 124^{6}, 125^{1}, 126^{4}, 127^{4}, 128^{3}, 129^{1}, 130^{2}, 131^{1}, 132^{6}, 133^{5}, 134^{5}, 135^{4}, 136^{5}, 137^{4}, 138^{7}, 139^{4}, 141^{7}, 142^{5}, 143^{4}, 144^{4}, 145^{3}, 146^{6}, 147^{5}, 148^{8}, 149^{5}, 150^{7}, 151^{6}, 152^{6}, 153^{10}, 154^{5}, 155^{5}, 156^{4}, 157^{3}, 158^{4}, 159^{3}, 160^{2}, 161^{2}, 162^{4}, 163^{2}, 165^{1}, 166^{3}, 167^{4}, 168^{3}, 169^{5}, 170^{2}, 171^{4}, 172^{4}, 173^{5}, 174^{5}, 175^{3}, 176^{8}, 177^{5}, 178^{3}, 179^{4}, 180^{2}, 181^{4}, 183^{1}, 184^{5}, 185^{1}, 186^{5}, 187^{3}, 188^{2}, 189^{3}, 190^{3}, 191^{5}, 192^{4}, 193^{1}, 195^{3}, 196^{2}, 197^{4}, 198^{5}, 199^{1}, 201^{2}, 202^{2}, 203^{2}, 204^{1}, 205^{3}, 206^{1}, 207^{1}, 208^{1}, 209^{2}, 210^{2}, 211^{2}, 212^{4}, 213^{2}, 214^{4}, 217^{2}, 218^{4}, 219^{2}, 220^{1}, 221^{2}, 222^{2}, 223^{2}, 224^{1}, 226^{1}, 227^{1}, 228^{1}, 229^{2}, 230^{1}, 231^{1}, 232^{1}, 233^{2}, 234^{1}, 235^{2}, 236^{1}, 237^{2}, 238^{2}, 239^{2}, 240^{3}, 241^{2}, 242^{4}, 243^{1}, 245^{2}, 246^{3}, 247^{2}, 248^{3}, 249^{5}, 250^{3}, 251^{4}, 252^{3}, 253^{2}, 254^{6}, 255^{1}, 257^{1}, 258^{1}, 259^{3}, 260^{1}, 262^{6}, 263^{5}, 264^{4}, 265^{3}, 266^{2}, 267^{7}, 268^{6}, 269^{7}, 270^{8}, 271^{7}, 273^{1}, 274^{1}, 275^{2}, 276^{5}, 277^{2}, 278^{4}, 279^{2}, 280^{7}, 281^{5}, 283^{2}, 284^{4}, 285^{6}, 286^{1}, 287^{1}, 288^{5}, 289^{2}, 290^{4}, 291^{2}, 294^{1}, 295^{3}, 297^{1}, 299^{1}, 301^{3}, 302^{1}, 303^{5}, 304^{4}, 305^{4}, 306^{4}, 307^{3}, 308^{7}, 309^{5}, 310^{4}, 311^{4}, 312^{3}, 313^{2}, 314^{2}, 315^{4}, 316^{3}, 317^{3}, 318^{4}, 319^{4}, 320^{8}, 321^{3}, 323^{2}, 324^{1}, 326^{2}, 327^{2}, 328^{1}, 329^{3}, 330^{1}, 331^{1}, 332^{2}, 333^{2}, 334^{2}, 335^{4}, 336^{2}, 337^{2}, 338^{1}, 341^{1}, 344^{1}, 345^{1}, 347^{2}, 349^{4}, 350^{2}, 351^{6}, 352^{7}, 353^{6}, 354^{1}, 355^{1}, 356^{1}, 357^{5}, 358^{2}, 359^{6}, 360^{5}, 363^{4}, 364^{3}, 365^{3}, 366^{2}, 367^{1}, 369^{2}, 370^{2}, 371^{1}, 372^{3}, 373^{1}, 374^{2}, 375^{4}, 376^{2}, 381^{6}, 383^{1}, 384^{5}, 385^{4}, 386^{2}, 387^{1}, 389^{2}, 390^{1}, 391^{3}, 392^{2}, 394^{4}, 395^{1}, 396^{2}, 397^{2}, 398^{1}, 399^{1}
3	(0, 0), (0, 1), (1, 0), (1, 1)	5^{1}, 13^{1}, 21^{1}, 28^{1}, 40^{1}, 43^{1}, 86^{1}, 87^{1}, 113^{1}, 120^{1}, 121^{1}, 130^{1}, 131^{1}, 163^{1}, 164^{1}, 171^{1}, 190^{1}, 197^{1}, 232^{1}, 274^{1}, 279^{1}, 302^{1}, 343^{1}, 356^{1}, 382^{1}
4	(0, 0), (1, 2), (2, 1)	58^{1}, 59^{1}

Ind.	2-face Vertices	Polytope$^{\text{Multiplicity}}$
5	(0, 0), (0, 3), (1, 0)	1^2, 4^1, 5^1, 6^1, 7^2, 8^1, 9^2, 10^2, 12^2, 13^2, 14^3, 15^1, 16^1, 17^1, 19^2, 23^1, 25^1, 26^1, 27^2, 30^2, 31^1, 32^1, 34^1, 36^1, 37^1, 42^1, 44^1, 46^1, 47^1, 48^1, 52^1, 53^1, 55^1, 63^1, 64^3, 65^4, 66^1, 67^1, 68^1, 69^1, 70^1, 71^1, 72^5, 73^1, 74^1, 79^4, 80^5, 81^4, 82^3, 83^6, 84^5, 89^1, 91^2, 92^1, 95^1, 97^1, 98^1, 100^2, 101^1, 103^1, 104^1, 106^2, 107^3, 108^4, 109^4, 110^2, 111^4, 112^4, 113^4, 114^2, 115^1, 116^2, 117^1, 119^1, 120^1, 127^1, 130^1, 132^1, 133^1, 136^1, 142^1, 144^1, 148^1, 149^1, 154^1, 155^1, 156^1, 159^1, 161^1, 162^1, 166^1, 167^1, 168^1, 170^2, 172^1, 173^1, 174^1, 175^1, 177^1, 180^2, 182^3, 183^1, 185^1, 187^1, 188^2, 193^4, 194^3, 195^3, 196^2, 199^1, 201^2, 202^2, 203^2, 204^1, 205^1, 206^3, 207^1, 208^1, 209^2, 210^2, 211^2, 212^2, 213^4, 214^2, 215^2, 219^1, 221^2, 222^1, 224^3, 225^2, 227^2, 229^1, 230^2, 231^1, 232^1, 233^2, 234^2, 235^1, 236^2, 239^2, 240^1, 241^1, 242^1, 244^2, 246^3, 247^2, 250^2, 255^1, 256^2, 257^1, 258^1, 259^1, 260^3, 261^2, 263^1, 265^1, 267^1, 269^1, 271^1, 272^1, 273^1, 274^1, 275^1, 276^1, 277^2, 278^2, 279^2, 280^1, 281^1, 282^2, 284^2, 291^3, 292^4, 293^5, 296^1, 297^2, 298^1, 299^1, 309^1, 315^1, 316^1, 321^1, 322^3, 323^2, 324^1, 326^2, 327^2, 328^1, 329^1, 330^3, 331^1, 332^2, 333^2, 334^4, 335^2, 337^1, 339^2, 341^2, 342^1, 344^1, 345^2, 346^1, 347^2, 348^2, 352^1, 355^1, 356^1, 357^1, 358^2, 360^1, 361^1, 365^1, 367^1, 369^2, 370^2, 371^1, 372^1, 373^3, 374^2, 375^2, 378^1, 380^1, 383^1, 384^1, 387^1, 388^2, 389^2, 390^1, 391^1, 392^2, 395^1, 397^2, 398^1, 399^1
6	(0, 0), (0, 2), (1, 0), (1, 1)	1^1, 6^1, 12^1, 18^1, 19^1, 36^2, 39^2, 51^2, 55^1, 56^1, 87^1, 94^1, 98^2, 104^2, 108^1, 110^1, 120^2, 124^1, 130^2, 131^2, 136^1, 137^1, 139^2, 140^1, 144^1, 145^1, 147^2, 159^1, 160^1, 163^2, 164^2, 165^1, 178^2, 191^1, 197^1, 228^1, 241^1, 249^1, 252^3, 255^2, 265^2, 266^2, 275^1, 290^1, 302^2, 305^1, 307^1, 313^1, 350^2, 354^1
7	(0, 0), (1, 2), (2, 0)	52^1, 66^1, 70^1, 71^1, 156^1, 157^1, 159^1, 160^1, 167^2, 169^2, 172^2, 183^1, 185^1, 187^1, 312^1, 313^1, 315^2, 317^2, 364^2
8	(0, 0), (0, 4), (1, 0)	3^1, 11^2, 28^2, 40^1, 41^1, 114^1, 115^1, 116^1, 123^1, 124^1, 133^1, 135^1, 136^1, 137^1, 162^1, 177^1, 207^2, 211^2, 220^2, 223^2, 297^1, 298^1, 304^1, 305^1, 331^2, 338^2, 361^1, 368^2, 377^2
9	(0, 0), (0, 2), (2, 0)	1^3, 2^3, 8^2, 11^2, 14^2, 15^2, 16^2, 18^1, 24^2, 25^2, 28^2, 29^2, 30^2, 31^2, 32^1, 33^1, 34^1, 35^1, 38^2, 41^2, 44^2, 45^2, 47^2, 48^2, 49^2, 50^3, 51^2, 52^1, 53^2, 54^2, 55^2, 56^2, 76^1, 77^1, 78^1, 87^1, 90^1, 96^2, 99^2, 102^2, 105^1, 121^1, 122^1, 126^4, 132^1, 134^1, 138^1, 141^1, 142^4, 143^4, 146^3, 147^1, 148^1, 149^4, 150^1, 151^4, 152^3, 153^5, 154^4, 155^2, 156^1, 157^1, 158^2, 159^1, 160^1, 168^1, 170^1, 171^2, 173^1, 174^2, 175^1, 176^4, 179^2, 180^1, 181^7, 184^1, 186^1, 192^5, 217^2, 238^1, 239^2, 240^2, 241^2, 242^2, 246^2, 247^2, 248^1, 249^1, 250^1, 251^3, 252^1, 253^1, 254^3, 255^1, 257^1, 258^1, 259^1, 262^3, 263^1, 264^1, 265^1, 266^1, 267^3, 268^3, 269^3, 270^3, 271^3, 276^2, 278^2, 280^2, 281^2, 284^2, 285^2, 286^1, 287^1, 288^2, 289^2, 290^2, 303^1, 306^4, 308^1, 309^4, 310^4, 311^2, 312^1, 313^1, 316^1, 318^1, 319^2, 320^4, 321^1, 347^2, 349^1, 350^1, 351^3, 352^3, 353^3, 357^2, 359^2, 360^2, 363^4, 365^1, 366^1, 381^3, 384^2, 385^2, 386^1, 394^2
10	(0, 0), (0, 1), (1, 0), (2, 2)	60^1, 62^1, 184^1

Ind.	2-face Vertices	Polytope$^{\text{Multiplicity}}$
11	(0, 0), (0, 3), (1, 0), (1, 1)	7^1, 17^1, 27^1, 30^1, 36^1, 46^2, 47^2, 85^1, 86^1, 91^1, 94^1, 95^3, 100^3, 101^3, 117^1, 118^1, 119^1, 120^2, 140^3, 163^1, 164^1, 178^1, 188^2, 189^1, 190^1, 191^1, 195^2, 196^2, 197^1, 215^3, 220^1, 223^2, 224^3, 225^3, 226^1, 234^2, 235^2, 236^2, 248^1, 249^1, 252^1, 255^1, 272^1, 296^3, 299^1, 300^1, 323^2, 338^1, 339^3, 345^2, 346^2, 362^1, 380^2
12	(0, 0), (0, 2), (1, 0), (1, 2)	242^1
13	(0, 0), (0, 5), (1, 0)	32^1, 33^1, 58^1, 59^1, 183^1, 185^1, 187^1, 208^2, 226^1, 286^1, 325^2, 340^1
14	(0, 0), (0, 1), (1, 2), (2, 0)	67^1, 73^1, 74^1, 76^1, 78^1, 86^1, 87^1, 189^1, 190^1, 191^1, 197^1
15	(0, 0), (0, 4), (1, 0), (1, 1)	3^1, 18^1, 20^1, 39^1, 40^1, 41^1, 117^1, 118^1, 119^1, 139^1, 144^1, 145^1, 163^1, 178^1, 299^1, 300^1, 307^1, 362^1
16	(0, 0), (0, 3), (1, 0), (1, 2)	37^1, 52^1, 239^1, 246^1, 247^1, 250^1, 255^1, 347^1
17	(0, 0), (1, 3), (2, 0)	105^1, 125^1, 129^1
18	(0, 0), (0, 6), (1, 0)	57^1, 182^1, 193^1, 194^1, 200^2, 237^1, 245^1, 322^1
19	(0, 0), (0, 3), (2, 0)	1^1, 2^1, 3^2, 4^3, 5^3, 6^3, 7^3, 8^2, 9^4, 10^4, 11^1, 12^4, 13^4, 14^2, 15^2, 16^2, 17^3, 18^2, 19^1, 20^1, 21^2, 22^2, 23^3, 25^1, 26^3, 27^3, 28^1, 29^1, 30^2, 31^2, 32^4, 33^3, 34^3, 35^2, 36^1, 37^3, 38^2, 39^1, 40^2, 41^1, 42^1, 43^2, 45^1, 46^1, 48^3, 49^2, 50^2, 51^2, 52^1, 53^3, 54^2, 55^3, 56^2, 57^1, 58^1, 59^1, 60^1, 61^1, 62^1, 63^3, 64^2, 65^3, 66^4, 67^3, 68^3, 69^3, 70^3, 71^3, 72^2, 73^2, 74^2, 75^1, 76^1, 77^1, 78^1, 79^3, 80^4, 81^3, 82^2, 83^3, 84^2, 85^3, 86^2, 87^1, 88^1, 89^2, 90^4, 91^2, 92^2, 93^1, 94^3, 95^2, 96^1, 97^2, 98^2, 99^6, 100^3, 101^2, 102^1, 103^1, 104^1, 105^1, 106^2, 107^2, 108^1, 109^2, 110^2, 111^1, 112^2, 113^2, 114^4, 115^3, 116^4, 117^3, 118^2, 119^3, 120^2, 121^1, 122^1, 123^1, 124^1, 125^2, 126^2, 127^3, 128^2, 129^2, 130^3, 131^2, 132^2, 133^2, 134^1, 135^1, 136^2, 137^1, 138^1, 139^1, 140^2, 141^2, 142^3, 143^2, 144^2, 145^1, 146^1, 147^1, 148^3, 149^3, 150^2, 151^2, 152^1, 154^3, 155^2, 156^2, 157^1, 158^1, 159^2, 160^1, 161^1, 162^1, 163^1, 164^1, 165^2, 166^3, 167^3, 168^5, 169^2, 170^4, 171^1, 172^3, 173^5, 174^2, 175^5, 177^1, 178^1, 179^2, 180^3, 181^1, 182^1, 183^1, 184^3, 185^1, 186^3, 187^1, 188^1, 189^1, 190^1, 191^1, 192^1, 193^2, 194^1, 195^2, 196^1, 197^1, 198^2, 199^3, 200^2, 201^4, 202^4, 203^4, 204^3, 205^3, 206^3, 207^3, 208^3, 209^4, 210^4, 211^4, 212^4, 213^4, 214^4, 215^1, 216^2, 218^2, 219^3, 220^3, 221^4, 222^3, 223^4, 224^2, 225^1, 226^3, 227^2, 228^2, 229^1, 230^2, 231^3, 232^3, 233^4, 234^2, 235^1, 236^2, 237^2, 238^3, 239^1, 240^2, 241^2, 242^2, 243^2, 244^2, 245^2, 246^2, 247^1, 248^2, 249^2, 250^1, 251^3, 252^2, 253^4, 254^3, 255^1, 256^3, 257^4, 258^3, 259^3, 260^4, 261^3, 262^1, 263^2, 264^1, 265^2, 266^1, 267^2, 268^1, 269^2, 270^1, 271^2, 272^2, 273^3, 274^3, 275^3, 276^2, 277^4, 278^1, 279^4, 280^2, 281^2, 282^2, 283^2, 284^1, 285^1, 286^3, 287^2, 288^2, 289^2, 290^2, 291^2, 292^3, 293^2, 294^1, 295^1, 296^2, 297^4, 298^3, 299^3, 300^2, 301^2, 302^2, 303^1, 304^1, 305^1, 306^2, 307^1, 308^2, 309^3, 310^2, 311^1, 312^1, 313^1, 314^2, 315^3, 316^5, 317^2, 318^4, 319^1, 321^5, 322^1, 323^1, 324^3, 325^2, 326^4, 327^4, 328^3, 329^3, 330^3, 331^3, 332^4, 333^4, 334^4, 335^4, 336^2, 337^3, 338^3, 339^1, 340^2, 341^2, 342^1, 343^2, 344^3, 345^2, 346^1, 347^1, 348^3, 349^1, 350^1, 351^1, 352^2, 353^1, 354^2, 355^3, 356^3, 357^2, 358^4, 359^1, 360^2, 361^3, 362^2, 363^2, 364^2, 365^5, 366^4, 367^3, 368^2, 369^4, 370^4, 371^3, 372^3, 373^3, 374^4, 375^4, 376^2, 377^2, 378^1, 379^2, 380^1, 381^1, 382^2, 383^3, 384^2, 385^1, 386^4, 387^3, 388^2, 389^4, 390^3, 391^3, 392^4, 393^2, 394^1, 395^3, 396^2, 397^4, 398^3, 399^3, 400^2, 401^2

Ind.	2-face Vertices	Polytope$^{\text{Multiplicity}}$
20	(0, 0), (0, 5), (1, 0), (1, 1)	34^1, 35^1, 60^1, 62^1, 226^1, 287^1, 340^1
21	(0, 0), (0, 2), (2, 0), (2, 1)	179^1, 192^1
22	(0, 0), (0, 4), (1, 0), (1, 2)	38^1, 51^1
23	(0, 0), (0, 7), (1, 0)	42^1, 44^1, 88^1, 89^1, 227^1, 229^1, 230^1, 294^1, 341^1, 342^1, 378^1
24	(0, 0), (0, 1), (1, 3), (2, 0)	127^1, 128^1, 130^1, 131^1, 301^1, 302^1
25	(0, 0), (0, 6), (1, 0), (1, 1)	61^1
26	(0, 0), (0, 3), (1, 2), (2, 0)	34^1, 35^1, 67^1, 71^1, 72^1, 73^2, 74^1, 83^1, 84^1, 86^1, 95^1, 100^1, 101^1, 103^1, 104^1, 117^1, 118^1, 119^1, 180^1, 258^1, 287^1, 293^1, 296^1, 299^1, 300^1, 362^1
27	(0, 0), (0, 5), (1, 0), (1, 2)	48^1, 49^1, 55^1, 56^1, 76^1, 78^1, 87^1, 189^1, 190^1, 191^1, 197^1, 288^1, 290^1
28	(0, 0), (0, 4), (2, 0)	18^1, 20^1, 23^1, 25^1, 38^1, 39^1, 50^2, 51^1, 63^1, 64^1, 68^1, 69^1, 79^1, 82^1, 85^1, 90^1, 91^1, 94^1, 99^2, 120^1, 123^1, 124^1, 126^1, 127^1, 128^1, 130^1, 131^1, 133^1, 135^1, 136^1, 137^1, 139^1, 142^1, 143^1, 144^1, 145^1, 149^1, 151^1, 154^1, 168^1, 170^1, 173^1, 175^1, 179^1, 180^1, 239^2, 240^2, 241^2, 242^2, 246^2, 247^2, 248^1, 249^1, 251^1, 252^1, 253^1, 254^1, 291^1, 301^1, 302^1, 304^1, 305^1, 306^1, 307^1, 309^1, 310^1, 316^1, 318^1, 321^1, 347^2, 363^1, 365^1, 366^1, 386^1
29	(0, 0), (1, 2), (2, 2), (3, 0)	198^1
30	(0, 0), (0, 2), (1, 3), (2, 0)	263^1, 264^1, 265^1, 266^1, 349^1, 350^1
31	(0, 0), (0, 6), (1, 0), (1, 2)	75^1, 77^1, 188^1, 195^1, 196^1, 237^1, 245^1, 323^1
32	(0, 0), (0, 3), (2, 0), (2, 1)	18^1, 38^1, 48^1, 49^1, 51^1, 55^1, 56^1, 70^1, 74^1, 86^1, 259^1, 288^1, 290^1
33	(0, 0), (0, 3), (3, 0)	17^1, 37^1, 65^2, 66^1, 67^1, 70^1, 71^1, 72^2, 73^1, 74^1, 80^2, 81^2, 83^2, 84^2, 86^1, 95^2, 100^2, 101^2, 107^1, 108^1, 109^1, 111^1, 112^1, 113^1, 114^1, 115^1, 116^1, 117^1, 118^1, 119^1, 140^1, 256^1, 260^1, 261^1, 292^2, 293^2, 296^2, 297^1, 298^1, 299^1, 300^1, 348^1, 361^1, 362^1
34	(0, 0), (0, 7), (1, 0), (1, 2)	92^1, 93^1, 295^1
35	(0, 0), (0, 6), (1, 0), (1, 3)	97^1, 98^1, 103^1, 104^1, 215^1, 224^1, 225^1, 339^1
36	(0, 0), (0, 10), (1, 0)	2^1, 26^1, 31^1, 179^1, 283^1, 285^1
37	(0, 0), (0, 5), (2, 0)	22^2, 23^1, 24^2, 25^1, 32^1, 33^1, 34^1, 35^1, 48^1, 49^1, 53^2, 54^2, 55^1, 56^1, 58^1, 60^1, 76^1, 125^1, 129^1, 141^1, 148^1, 150^1, 167^1, 169^1, 172^1, 216^2, 217^2, 250^1, 263^1, 264^1, 286^1, 287^1, 288^1, 289^2, 290^1, 308^1, 315^1, 317^1, 349^1, 364^1
38	(0, 0), (0, 1), (1, 3), (3, 0)	161^1, 164^1
39	(0, 0), (0, 4), (2, 0), (2, 1)	248^1
40	(0, 0), (0, 3), (2, 0), (2, 2)	50^1, 53^1, 54^1, 289^1
41	(0, 0), (0, 7), (1, 0), (1, 3)	19^1, 36^1, 46^1, 47^1, 234^1, 235^1, 236^1, 345^1, 346^1, 380^1
42	(0, 0), (0, 6), (1, 0), (1, 4)	123^1, 124^1, 139^1
43	(0, 0), (0, 11), (1, 0)	22^2, 23^2
44	(0, 0), (0, 10), (1, 0), (1, 1)	21^1, 29^1
45	(0, 0), (0, 5), (1, 3), (2, 0)	59^1, 62^1, 78^1, 87^1, 255^1, 265^1, 266^1, 350^1
46	(0, 0), (0, 7), (1, 0), (1, 4)	133^1, 135^1, 136^1, 137^1, 144^1, 145^1, 304^1, 305^1, 307^1
47	(0, 0), (0, 4), (1, 3), (2, 0), (2, 1)	249^1, 252^1
48	(0, 0), (0, 12), (1, 0)	216^2, 219^1, 221^1, 244^1, 337^1, 376^1
49	(0, 0), (0, 4), (3, 0)	63^1, 64^1, 68^1, 69^1, 79^1, 82^1, 114^1, 115^1, 116^1, 117^1, 118^1, 119^1, 291^1, 297^1, 298^1, 299^1, 300^1, 361^1, 362^1

Ind.	2-face Vertices	Polytope$^{\text{Multiplicity}}$
50	(0, 0), (0, 6), (2, 0)	1^1, 2^2, 4^1, 5^1, 6^1, 7^1, 8^1, 9^2, 10^2, 12^2, 13^2, 14^1, 15^1, 16^1, 21^2, 26^2, 27^1, 29^2, 30^1, 31^2, 32^1, 34^1, 48^1, 53^1, 55^1, 57^1, 61^1, 75^1, 77^1, 79^1, 80^1, 83^1, 89^1, 92^1, 96^2, 97^1, 98^1, 100^1, 102^2, 103^1, 104^1, 114^1, 116^1, 117^1, 119^1, 121^1, 122^1, 123^1, 124^1, 127^1, 130^1, 132^1, 133^1, 136^1, 138^1, 139^1, 142^1, 144^1, 146^1, 147^1, 148^1, 149^1, 152^1, 153^1, 154^1, 155^1, 156^1, 159^1, 166^1, 167^1, 168^1, 172^1, 173^1, 174^1, 175^1, 179^1, 193^1, 195^1, 199^1, 201^2, 202^2, 203^2, 204^1, 205^1, 206^1, 207^1, 208^1, 209^2, 210^2, 211^2, 212^2, 213^2, 214^2, 218^2, 219^2, 220^1, 221^2, 222^2, 223^2, 224^1, 226^1, 227^1, 230^1, 231^1, 232^1, 233^2, 234^1, 236^1, 246^1, 260^1, 262^1, 263^1, 265^1, 267^2, 268^1, 269^2, 270^1, 271^2, 273^1, 274^1, 275^1, 276^1, 277^2, 279^2, 280^1, 281^1, 283^2, 285^2, 297^1, 299^1, 309^1, 315^1, 316^1, 321^1, 324^1, 326^2, 327^2, 328^1, 329^1, 330^1, 331^1, 332^2, 333^2, 334^2, 335^2, 336^2, 337^2, 338^1, 341^1, 344^1, 345^1, 351^1, 352^2, 353^1, 355^1, 356^1, 357^1, 358^2, 360^1, 365^1, 367^1, 369^2, 370^2, 371^1, 372^1, 373^1, 374^2, 375^2, 376^2, 381^1, 383^1, 384^1, 387^1, 389^2, 390^1, 391^1, 392^2, 395^1, 397^2, 398^1, 399^1
51	(0, 0), (0, 5), (2, 0), (2, 1)	250^1, 255^1, 263^1, 264^1, 265^1, 266^1, 349^1, 350^1
52	(0, 0), (0, 4), (2, 0), (2, 2)	251^1
53	(0, 0), (0, 12), (1, 0), (1, 1)	222^1, 336^1
54	(0, 0), (0, 4), (1, 3), (3, 0)	85^1, 91^1, 94^1, 120^1, 127^1, 128^1, 130^1, 131^1, 162^1, 163^1, 301^1, 302^1
55	(0, 0), (0, 7), (2, 0)	1^1, 3^2, 4^1, 5^1, 6^1, 7^1, 8^1, 11^2, 14^1, 15^1, 16^1, 17^1, 18^1, 19^1, 20^1, 27^1, 28^2, 30^1, 33^1, 35^1, 36^1, 37^1, 38^1, 39^1, 40^2, 41^2, 42^1, 43^2, 44^1, 45^2, 46^1, 47^1, 49^1, 50^1, 51^1, 52^1, 54^1, 56^1, 57^1, 58^1, 59^1, 60^1, 61^1, 62^1, 63^1, 64^1, 65^1, 66^1, 67^1, 68^1, 69^1, 70^1, 71^1, 72^1, 73^1, 74^1, 75^1, 76^1, 77^1, 78^1, 81^1, 82^1, 84^1, 85^1, 86^1, 87^1, 88^2, 89^1, 90^1, 91^1, 92^1, 93^2, 94^1, 95^1, 96^1, 97^1, 98^1, 101^1, 102^1, 103^1, 104^1, 105^1, 106^1, 107^1, 108^1, 109^1, 110^1, 111^1, 112^1, 113^1, 115^1, 118^1, 120^1, 121^1, 122^1, 123^1, 124^1, 125^1, 126^1, 128^1, 129^1, 131^1, 132^1, 133^1, 134^2, 135^2, 136^1, 137^2, 138^1, 139^1, 140^1, 141^1, 143^1, 144^1, 145^2, 146^1, 147^1, 150^1, 151^1, 152^1, 153^1, 155^1, 156^1, 157^2, 158^2, 159^1, 160^2, 161^1, 162^1, 163^1, 164^1, 165^2, 166^1, 169^1, 170^1, 171^2, 174^1, 176^2, 177^1, 178^1, 180^1, 181^1, 182^1, 183^1, 184^1, 185^1, 186^1, 187^1, 188^1, 189^1, 190^1, 191^1, 192^1, 194^1, 196^1, 197^1, 198^1, 199^1, 200^2, 204^1, 205^1, 206^1, 207^1, 208^1, 215^1, 220^1, 225^1, 226^1, 228^2, 229^1, 231^1, 232^1, 235^1, 237^2, 238^1, 239^1, 240^1, 241^1, 242^1, 247^1, 248^1, 249^1, 250^1, 251^1, 252^1, 253^1, 254^1, 255^1, 256^1, 257^1, 258^1, 259^1, 261^1, 262^1, 264^1, 266^1, 268^1, 270^1, 272^2, 273^1, 274^1, 275^1, 276^1, 278^2, 280^1, 281^1, 282^2, 284^2, 286^1, 287^1, 288^1, 289^1, 290^1, 291^1, 292^1, 293^1, 294^2, 295^2, 296^1, 298^1, 300^1, 301^1, 302^1, 303^2, 304^2, 305^2, 306^1, 307^2, 308^1, 310^1, 311^2, 312^2, 313^2, 314^2, 317^1, 318^1, 319^2, 320^2, 322^1, 323^1, 324^1, 325^2, 328^1, 329^1, 330^1, 331^1, 338^1, 339^1, 340^2, 342^1, 343^2, 344^1, 346^1, 347^1, 348^1, 349^1, 350^1, 351^1, 353^1, 354^2, 355^1, 356^1, 357^1, 359^2, 360^1, 361^1, 362^1, 363^1, 364^1, 366^1, 367^1, 368^2, 371^1, 372^1, 373^1, 377^2, 378^1, 379^2, 380^1, 381^1, 382^2, 383^1, 384^1, 385^2, 386^1, 387^1, 388^2, 390^1, 391^1, 393^2, 394^2, 395^1, 396^2, 398^1, 399^1, 400^2, 401^2

Ind.	2-face Vertices	Polytope$^{\text{Multiplicity}}$
56	(0, 0), (0, 6), (1, 4), (2, 0)	122^1, 244^2
57	(0, 0), (0, 6), (2, 0), (2, 1)	121^1
58	(0, 0), (0, 12), (1, 0), (1, 2)	218^1
59	(0, 0), (0, 4), (2, 2), (3, 0)	25^1, 90^1, 99^2, 126^1, 142^1, 143^1, 149^1, 151^1, 154^1, 168^1, 170^1, 173^1, 175^1, 177^1, 178^1, 179^1, 180^1, 253^1, 254^1, 306^1, 309^1, 310^1, 316^1, 318^1, 321^1, 363^1, 365^1, 366^1, 386^1
60	(0, 0), (0, 5), (3, 0)	125^1, 129^1, 183^1, 189^1
61	(0, 0), (0, 7), (1, 4), (2, 0)	132^1, 134^1, 245^2, 303^1
62	(0, 0), (0, 4), (3, 0), (3, 1)	23^1
63	(0, 0), (0, 6), (1, 4), (2, 0), (2, 1)	138^1, 147^1
64	(0, 0), (0, 8), (2, 0)	243^2
65	(0, 0), (0, 5), (2, 2), (3, 0)	141^1, 148^1, 150^1, 167^1, 169^1, 172^1, 185^1, 190^1, 308^1, 315^1, 317^1, 364^1
66	(0, 0), (0, 7), (2, 0), (2, 1)	156^1, 157^1, 159^1, 160^1, 312^1, 313^1
67	(0, 0), (0, 6), (2, 0), (2, 2)	1^1, 2^1, 146^1, 152^1, 153^1, 262^1, 267^1, 268^1, 269^1, 270^1, 271^1, 351^1, 352^1, 353^1, 381^1
68	(0, 0), (0, 5), (2, 0), (3, 1)	24^2, 25^1, 217^2
69	(0, 0), (0, 5), (1, 4), (3, 0)	187^1, 191^1, 197^1
70	(0, 0), (0, 6), (3, 0)	4^1, 5^1, 6^1, 7^1, 8^1, 9^2, 10^2, 12^2, 13^2, 14^1, 15^1, 16^1, 26^1, 27^1, 30^1, 31^1, 32^1, 34^1, 48^1, 53^1, 55^1, 79^1, 80^1, 83^1, 89^1, 92^1, 100^1, 114^1, 116^1, 117^1, 119^1, 127^1, 130^1, 132^1, 133^1, 136^1, 142^1, 144^1, 148^1, 149^1, 154^1, 155^1, 156^1, 159^1, 166^1, 167^1, 168^1, 172^1, 173^1, 174^1, 175^1, 182^1, 188^1, 193^2, 194^1, 195^2, 196^1, 199^1, 201^2, 202^2, 203^2, 204^1, 205^1, 206^1, 207^1, 208^1, 209^2, 210^2, 211^2, 212^2, 213^2, 214^2, 215^1, 219^1, 220^1, 221^2, 222^1, 223^2, 224^2, 225^1, 226^1, 227^1, 230^1, 231^1, 232^1, 233^2, 234^1, 236^1, 244^2, 246^1, 260^1, 263^1, 265^1, 267^1, 269^1, 271^1, 273^1, 274^1, 275^1, 276^1, 277^2, 279^2, 280^1, 281^1, 297^1, 299^1, 309^1, 315^1, 316^1, 321^1, 322^1, 323^1, 324^1, 326^2, 327^2, 328^1, 329^1, 330^1, 331^1, 332^2, 333^2, 334^2, 335^2, 337^1, 338^1, 339^1, 341^1, 344^1, 345^1, 352^1, 355^1, 356^1, 357^1, 358^2, 360^1, 365^1, 367^1, 369^2, 370^2, 371^1, 372^1, 373^1, 374^2, 375^2, 383^1, 384^1, 387^1, 389^2, 390^1, 391^1, 392^2, 395^1, 397^2, 398^1, 399^1
71	(0, 0), (0, 5), (3, 0), (3, 1)	22^2, 23^1, 216^2
72	(0, 0), (0, 7), (2, 0), (2, 2)	8^1, 11^1, 14^1, 15^1, 16^1, 19^1, 28^1, 36^1, 44^1, 45^1, 47^1, 153^1, 155^1, 158^1, 171^1, 174^1, 176^2, 254^1, 276^1, 278^1, 280^1, 281^1, 311^1, 319^1, 320^2, 357^1, 359^1, 360^1, 384^1, 385^1, 394^1
73	(0, 0), (0, 6), (1, 5), (2, 0), (2, 2)	29^1, 31^1, 285^1
74	(0, 0), (0, 7), (1, 5), (2, 0), (2, 2)	30^1, 41^1, 284^1
75	(0, 0), (0, 10), (2, 0)	2^1, 21^1, 26^1, 29^1, 31^1, 179^1, 283^1, 285^1

Ind.	2-face Vertices	Polytope$^{\text{Multiplicity}}$
76	(0, 0), (0, 7), (3, 0)	3^2, 4^1, 5^1, 6^1, 7^1, 11^1, 17^1, 18^1, 19^1, 20^1, 33^1, 35^1, 36^1, 37^1, 38^1, 39^1, 42^2, 43^2, 44^1, 45^1, 46^2, 47^1, 49^1, 50^1, 51^1, 52^1, 54^1, 56^1, 57^1, 58^1, 59^1, 60^1, 61^1, 62^1, 63^1, 64^1, 65^1, 66^1, 67^1, 68^1, 69^1, 70^1, 71^1, 72^1, 73^1, 74^1, 75^1, 76^1, 77^1, 78^1, 81^1, 82^1, 84^1, 85^1, 86^1, 87^1, 88^1, 90^1, 91^1, 93^1, 94^1, 95^1, 96^1, 97^1, 98^1, 101^1, 102^1, 103^1, 104^1, 105^1, 106^1, 107^1, 108^1, 109^1, 110^1, 111^1, 112^1, 113^1, 115^1, 118^1, 120^1, 121^1, 122^1, 123^1, 124^1, 125^1, 126^1, 128^1, 129^1, 131^1, 134^1, 135^1, 137^1, 138^1, 139^1, 140^1, 141^1, 143^1, 145^1, 146^1, 147^1, 150^1, 151^1, 152^1, 157^1, 158^1, 160^1, 161^1, 162^1, 163^1, 164^1, 165^2, 166^1, 169^1, 170^1, 171^1, 177^1, 178^1, 181^1, 182^1, 183^1, 184^1, 185^1, 186^1, 187^1, 188^1, 189^1, 190^1, 191^1, 192^1, 194^1, 196^1, 197^1, 198^1, 199^1, 200^2, 204^1, 205^1, 206^1, 207^1, 208^1, 215^1, 225^1, 227^1, 228^2, 229^2, 230^1, 231^1, 232^1, 234^1, 235^2, 236^1, 238^1, 239^1, 240^1, 241^1, 242^1, 247^1, 248^1, 249^1, 250^1, 251^1, 252^1, 253^1, 255^1, 256^1, 257^1, 258^1, 259^1, 261^1, 262^1, 264^1, 266^1, 268^1, 270^1, 272^2, 273^1, 274^1, 275^1, 278^1, 286^1, 287^1, 288^1, 289^1, 290^1, 291^1, 292^1, 293^1, 294^1, 295^1, 296^1, 298^1, 300^1, 301^1, 302^1, 303^1, 304^1, 305^1, 306^1, 307^1, 308^1, 310^1, 311^1, 312^1, 313^1, 314^2, 317^1, 318^1, 319^1, 322^1, 323^1, 324^1, 325^2, 328^1, 329^1, 330^1, 331^1, 339^1, 341^1, 342^2, 343^2, 344^1, 345^1, 346^2, 347^1, 348^1, 349^1, 350^1, 351^1, 353^1, 354^2, 355^1, 356^1, 359^1, 361^1, 362^1, 363^1, 364^1, 366^1, 367^1, 368^2, 371^1, 372^1, 373^1, 378^2, 379^2, 380^2, 381^1, 382^2, 383^1, 385^1, 386^1, 387^1, 388^2, 390^1, 391^1, 393^2, 394^1, 395^1, 396^2, 398^1, 399^1, 400^2, 401^2
77	(0, 0), (0, 6), (1, 5), (3, 0)	2^1, 21^2, 26^1, 29^1, 179^1, 218^2, 219^1, 222^1, 283^2, 285^1, 336^2, 337^1, 376^2
78	(0, 0), (0, 7), (1, 5), (3, 0)	1^1, 27^1, 28^1, 40^2, 41^1, 180^1, 220^1, 226^1, 237^2, 245^2, 282^2, 284^1, 338^1, 340^2, 377^2
79	(0, 0), (0, 8), (3, 0)	243^2
80	(0, 0), (0, 12), (2, 0)	218^1, 219^1, 221^1, 222^1, 336^1, 337^1, 376^1
81	(0, 0), (0, 26), (1, 0)	24^1, 25^1
82	(0, 0), (0, 28), (1, 0)	217^1
83	(0, 0), (0, 12), (3, 0)	244^1
84	(0, 0), (0, 26), (2, 0)	24^1, 25^1
85	(0, 0), (0, 28), (2, 0)	217^1
86	(0, 0), (0, 46), (2, 0)	1^1, 2^1, 3^1, 4^1, 5^1, 6^1, 7^1, 8^1, 9^1, 10^1, 11^1, 12^1, 13^1, 14^1, 15^1, 16^1, 21^1, 26^1, 27^1, 28^1, 29^1, 30^1, 31^1, 40^1, 41^1
87	(0, 0), (0, 48), (2, 0)	17^1, 18^1, 32^1, 33^1, 34^1, 35^1, 37^1, 38^1, 48^1, 49^1, 50^1, 51^1, 53^1, 54^1, 55^1, 56^1, 63^1, 64^1, 65^1, 66^1, 67^1, 68^1, 69^1, 70^1, 71^1, 72^1, 73^1, 74^1, 79^1, 80^1, 81^1, 82^1, 83^1, 84^1, 85^1, 86^1, 90^1, 91^1, 94^1, 95^1, 99^1, 100^1, 101^1, 114^1, 115^1, 116^1, 117^1, 118^1, 119^1, 120^1, 125^1, 126^1, 127^1, 128^1, 129^1, 130^1, 131^1, 141^1, 142^1, 143^1, 148^1, 149^1, 150^1, 151^1, 154^1, 167^1, 168^1, 169^1, 170^1, 172^1, 173^1, 175^1, 179^1, 180^1, 199^1, 200^1, 201^1, 202^1, 203^1, 204^1, 205^1, 206^1, 207^1, 208^1, 209^1, 210^1, 211^1, 212^1, 213^1, 214^1, 218^1, 219^1, 220^1, 221^1, 222^1, 223^1, 226^1, 237^1, 243^1, 244^1, 245^1
88	(0, 0), (0, 49), (2, 0)	42^1, 44^1
89	(0, 0), (0, 49), (1, 25), (2, 0)	19^1, 36^1, 46^1, 47^1

Ind.	2-face Vertices	Polytope$^{\text{Multiplicity}}$
90	(0, 0), (0, 50), (2, 0)	20^1, 39^1, 57^1, 58^1, 59^1, 60^1, 61^1, 62^1, 75^1, 76^1, 77^1, 78^1, 87^1, 88^1, 89^1, 92^1, 93^1, 96^1, 97^1, 98^1, 102^1, 103^1, 104^1, 121^1, 122^1, 123^1, 124^1, 132^1, 133^1, 134^1, 135^1, 136^1, 137^1, 138^1, 139^1, 144^1, 145^1, 146^1, 147^1, 152^1, 153^1, 155^1, 156^1, 157^1, 158^1, 159^1, 160^1, 165^1, 166^1, 171^1, 174^1, 176^1
91	(0, 0), (0, 49), (2, 0), (2, 1)	43^1, 45^1
92	(0, 0), (0, 51), (2, 0)	52^1, 107^1, 111^1, 112^1, 162^1, 177^1, 182^1, 183^1, 185^1, 187^1, 193^1, 194^1, 227^1, 229^1, 230^1
93	(0, 0), (0, 51), (1, 26), (2, 0)	108^1, 109^1, 113^1, 140^1, 163^1, 178^1, 188^1, 189^1, 190^1, 191^1, 195^1, 196^1, 197^1, 215^1, 224^1, 225^1, 234^1, 235^1, 236^1
94	(0, 0), (0, 52), (2, 0)	105^1, 106^1, 110^1, 161^1, 164^1, 181^1, 184^1, 192^1, 239^1, 240^1, 241^1, 242^1, 246^1, 247^1, 248^1, 249^1, 250^1, 251^1, 252^1, 253^1, 254^1, 255^1, 262^1, 263^1, 264^1, 265^1, 266^1, 267^1, 268^1, 269^1, 270^1, 271^1, 272^1, 273^1, 274^1, 275^1, 276^1, 277^1, 278^1, 279^1, 280^1, 281^1, 282^1, 283^1, 284^1, 285^1
95	(0, 0), (0, 51), (2, 0), (2, 1)	228^1, 231^1, 232^1, 233^1
96	(0, 0), (0, 53), (2, 0)	186^1, 198^1
97	(0, 0), (0, 54), (2, 0)	238^1, 256^1, 257^1, 258^1, 259^1, 260^1, 261^1, 286^1, 287^1, 288^1, 289^1, 290^1, 291^1, 292^1, 293^1, 296^1, 297^1, 298^1, 299^1, 300^1, 301^1, 302^1, 306^1, 308^1, 309^1, 310^1, 315^1, 316^1, 317^1, 318^1, 321^1, 324^1, 325^1, 326^1, 327^1, 328^1, 329^1, 330^1, 331^1, 332^1, 333^1, 334^1, 335^1, 336^1, 337^1, 338^1, 340^1
98	(0, 0), (0, 56), (2, 0)	22^1, 23^1, 24^1, 25^1, 294^1, 295^1, 303^1, 304^1, 305^1, 307^1, 311^1, 312^1, 313^1, 314^1, 319^1, 320^1
99	(0, 0), (0, 57), (2, 0)	322^1, 341^1, 342^1
100	(0, 0), (0, 57), (1, 29), (2, 0)	323^1, 339^1, 345^1, 346^1
101	(0, 0), (0, 58), (2, 0)	347^1, 349^1, 350^1, 351^1, 352^1, 353^1, 354^1, 355^1, 356^1, 357^1, 358^1, 359^1, 360^1
102	(0, 0), (0, 57), (2, 0), (2, 1)	343^1, 344^1
103	(0, 0), (0, 60), (2, 0)	216^1, 217^1, 348^1, 361^1, 362^1, 363^1, 364^1, 365^1, 366^1, 367^1, 368^1, 369^1, 370^1, 371^1, 372^1, 373^1, 374^1, 375^1, 376^1, 377^1
104	(0, 0), (0, 63), (2, 0)	378^1
105	(0, 0), (0, 63), (1, 32), (2, 0)	380^1
106	(0, 0), (0, 64), (2, 0)	381^1, 382^1, 383^1, 384^1, 385^1
107	(0, 0), (0, 63), (2, 0), (2, 1)	379^1
108	(0, 0), (0, 66), (2, 0)	386^1, 387^1, 388^1, 389^1, 390^1, 391^1, 392^1
109	(0, 0), (0, 70), (2, 0)	393^1, 394^1
110	(0, 0), (0, 46), (2, 16), (3, 0)	1^1, 2^1, 8^1, 11^1, 14^1, 15^1, 16^1, 28^1, 29^1, 30^1, 31^1, 41^1
111	(0, 0), (0, 46), (3, 0), (3, 1)	3^1, 4^1, 5^1, 6^1, 7^1, 9^1, 10^1, 12^1, 13^1, 21^1, 26^1, 27^1, 40^1
112	(0, 0), (0, 72), (2, 0)	395^1, 396^1, 397^1, 398^1
113	(0, 0), (0, 48), (3, 0)	17^1, 18^1, 32^1, 33^1, 34^1, 35^1, 37^1, 38^1, 48^1, 49^1, 50^1, 51^1, 53^1, 54^1, 55^1, 56^1, 63^1, 64^1, 65^1, 66^1, 67^1, 68^1, 69^1, 70^1, 71^1, 72^1, 73^1, 74^1, 79^1, 80^1, 81^1, 82^1, 83^1, 84^1, 85^1, 86^1, 90^1, 91^1, 94^1, 95^1, 99^1, 100^1, 101^1, 114^1, 115^1, 116^1, 117^1, 118^1, 119^1, 120^1, 125^1, 126^1, 127^1, 128^1, 129^1, 130^1, 131^1, 141^1, 142^1, 143^1, 148^1, 149^1, 150^1, 151^1, 154^1, 167^1, 168^1, 169^1, 170^1, 172^1, 173^1, 175^1, 179^1, 180^1, 199^1, 200^1, 201^1, 202^1, 203^1, 204^1, 205^1, 206^1, 207^1, 208^1, 209^1, 210^1, 211^1, 212^1, 213^1, 214^1, 218^1, 219^1, 220^1, 221^1, 222^1, 223^1, 226^1, 237^1, 243^1, 244^1, 245^1
114	(0, 0), (0, 49), (2, 17), (3, 0)	19^1, 36^1, 44^1, 45^1, 47^1

Ind.	2-face Vertices	Polytope$^{\text{Multiplicity}}$
115	(0, 0), (0, 50), (3, 0)	57^1, 58^1, 59^1, 88^1, 89^1
116	(0, 0), (0, 49), (3, 0), (3, 1)	42^1, 43^1, 46^1
117	(0, 0), (0, 50), (2, 17), (3, 0)	20^1, 60^1, 61^1, 62^1, 75^1, 92^1, 93^1
118	(0, 0), (0, 50), (1, 34), (3, 0)	39^1, 76^1, 77^1, 78^1, 87^1, 97^1, 98^1, 103^1, 104^1, 123^1, 124^1, 133^1, 135^1, 136^1, 137^1, 139^1, 144^1, 145^1
119	(0, 0), (0, 51), (3, 0)	52^1, 107^1, 108^1, 109^1, 111^1, 112^1, 113^1, 140^1, 162^1, 163^1, 177^1, 178^1, 182^1, 183^1, 185^1, 187^1, 188^1, 189^1, 190^1, 191^1, 193^1, 194^1, 195^1, 196^1, 197^1, 215^1, 224^1, 225^1, 227^1, 228^1, 229^1, 230^1, 231^1, 232^1, 233^1, 234^1, 235^1, 236^1
120	(0, 0), (0, 50), (2, 18), (3, 0)	96^1, 102^1, 121^1, 122^1, 132^1, 134^1, 138^1, 146^1, 147^1, 155^1, 156^1, 157^1, 158^1, 159^1, 160^1
121	(0, 0), (0, 50), (2, 0), (2, 18), (3, 1)	153^1, 176^1
122	(0, 0), (0, 50), (2, 18), (3, 0), (3, 1)	152^1, 171^1, 174^1
123	(0, 0), (0, 52), (3, 0)	105^1, 106^1, 110^1
124	(0, 0), (0, 78), (2, 0)	399^1, 400^1
125	(0, 0), (0, 50), (3, 0), (3, 2)	165^1, 166^1
126	(0, 0), (0, 52), (1, 35), (3, 0)	161^1, 164^1
127	(0, 0), (0, 52), (2, 18), (3, 0)	181^1, 184^1, 192^1, 239^1, 240^1, 241^1, 242^1, 246^1, 247^1, 248^1, 249^1, 250^1, 251^1, 252^1, 254^1, 255^1, 262^1, 263^1, 264^1, 265^1, 266^1, 267^1, 268^1, 269^1, 270^1, 271^1, 276^1, 278^1, 280^1, 281^1, 284^1, 285^1
128	(0, 0), (0, 52), (3, 0), (3, 1)	253^1, 272^1, 273^1, 274^1, 275^1, 277^1, 279^1, 282^1, 283^1
129	(0, 0), (0, 53), (2, 18), (3, 0)	186^1, 198^1
130	(0, 0), (0, 54), (3, 0)	238^1, 256^1, 257^1, 258^1, 259^1, 260^1, 261^1, 286^1, 287^1, 288^1, 289^1, 290^1, 291^1, 292^1, 293^1, 296^1, 297^1, 298^1, 299^1, 300^1, 301^1, 302^1, 306^1, 308^1, 309^1, 310^1, 315^1, 316^1, 317^1, 318^1, 321^1, 324^1, 325^1, 326^1, 327^1, 328^1, 329^1, 330^1, 331^1, 332^1, 333^1, 334^1, 335^1, 336^1, 337^1, 338^1, 340^1
131	(0, 0), (0, 56), (2, 0), (2, 26)	24^1, 25^1
132	(0, 0), (0, 56), (3, 0)	294^1
133	(0, 0), (0, 84), (2, 0)	401^1
134	(0, 0), (0, 56), (2, 19), (3, 0)	295^1
135	(0, 0), (0, 56), (1, 38), (3, 0)	304^1, 305^1, 307^1
136	(0, 0), (0, 57), (3, 0)	322^1, 323^1, 339^1, 341^1, 342^1, 343^1, 344^1, 345^1, 346^1
137	(0, 0), (0, 56), (2, 20), (3, 0)	303^1, 311^1, 312^1, 313^1
138	(0, 0), (0, 56), (2, 0), (2, 20), (3, 1)	320^1
139	(0, 0), (0, 56), (2, 20), (3, 0), (3, 1)	319^1
140	(0, 0), (0, 56), (3, 0), (3, 2)	314^1
141	(0, 0), (0, 58), (2, 20), (3, 0)	347^1, 349^1, 350^1, 351^1, 352^1, 353^1, 357^1, 359^1, 360^1
142	(0, 0), (0, 60), (2, 0), (2, 28)	217^1
143	(0, 0), (0, 58), (3, 0), (3, 1)	354^1, 355^1, 356^1, 358^1
144	(0, 0), (0, 60), (3, 0)	348^1, 361^1, 362^1, 363^1, 364^1, 365^1, 366^1, 367^1, 368^1, 369^1, 370^1, 371^1, 372^1, 373^1, 374^1, 375^1, 376^1, 377^1
145	(0, 0), (0, 63), (3, 0)	378^1, 379^1, 380^1
146	(0, 0), (0, 64), (2, 22), (3, 0)	381^1, 384^1, 385^1
147	(0, 0), (0, 64), (3, 0), (3, 1)	382^1, 383^1
148	(0, 0), (0, 66), (3, 0)	386^1, 387^1, 388^1, 389^1, 390^1, 391^1, 392^1
149	(0, 0), (0, 56), (3, 0), (3, 11)	22^1, 23^1
150	(0, 0), (0, 70), (2, 24), (3, 0)	394^1
151	(0, 0), (0, 70), (3, 0), (3, 1)	393^1
152	(0, 0), (0, 72), (3, 0)	395^1, 396^1, 397^1, 398^1

Ind.	2-face Vertices	Polytope$^{\text{Multiplicity}}$
153	(0, 0), (0, 60), (3, 0), (3, 12)	216^1
154	(0, 0), (0, 78), (3, 0)	399^1, 400^1
155	(0, 0), (0, 84), (3, 0)	401^1
156	(0, 0), (0, 56), (4, 12), (5, 0)	23^1, 25^1
157	(0, 0), (0, 56), (5, 0), (5, 1)	22^1, 24^1
158	(0, 0), (0, 60), (5, 0)	216^1, 217^1
159	(0, 0), (0, 46), (6, 0), (6, 10)	2^1, 21^1, 26^1, 29^1, 31^1
160	(0, 0), (0, 49), (7, 0)	19^1, 36^1, 42^1, 43^1, 44^1, 45^1, 46^1, 47^1
161	(0, 0), (0, 46), (6, 10), (7, 0)	4^1, 8^1
162	(0, 0), (0, 46), (6, 0), (6, 10), (7, 1)	10^1
163	(0, 0), (0, 46), (6, 0), (6, 10), (7, 2)	9^1
164	(0, 0), (0, 46), (6, 10), (7, 0), (7, 1)	5^1, 16^1
165	(0, 0), (0, 46), (6, 0), (6, 10), (7, 1), (7, 2)	13^1
166	(0, 0), (0, 46), (6, 10), (7, 0), (7, 2)	6^1, 15^1
167	(0, 0), (0, 46), (6, 0), (6, 10), (7, 1), (7, 3)	12^1
168	(0, 0), (0, 46), (6, 10), (7, 0), (7, 3)	1^1, 7^1, 14^1, 27^1, 30^1
169	(0, 0), (0, 46), (7, 0), (7, 4)	3^1, 11^1, 28^1, 40^1, 41^1
170	(0, 0), (0, 48), (2, 36), (6, 8), (7, 0)	18^1, 38^1, 50^1, 51^1
171	(0, 0), (0, 48), (2, 36), (6, 0), (7, 1)	32^1, 34^1, 48^1, 53^1, 55^1
172	(0, 0), (0, 48), (2, 36), (7, 0), (7, 1)	33^1, 35^1, 49^1, 54^1, 56^1
173	(0, 0), (0, 50), (4, 22), (7, 0)	20^1, 39^1
174	(0, 0), (0, 50), (5, 15), (7, 0)	58^1, 59^1, 60^1, 62^1, 76^1, 78^1, 87^1
175	(0, 0), (0, 50), (6, 8), (7, 0)	57^1, 61^1, 75^1, 77^1, 89^1, 92^1, 96^1, 97^1, 98^1, 102^1, 103^1, 104^1, 121^1, 122^1, 123^1, 124^1, 132^1, 133^1, 136^1, 138^1, 139^1, 144^1, 146^1, 147^1, 152^1, 153^1, 155^1, 156^1, 159^1, 166^1, 174^1
176	(0, 0), (0, 48), (4, 24), (6, 0), (6, 10)	179^1
177	(0, 0), (0, 50), (7, 0), (7, 1)	88^1, 93^1, 134^1, 135^1, 137^1, 145^1, 157^1, 158^1, 160^1, 165^1, 171^1, 176^1
178	(0, 0), (0, 48), (3, 30), (4, 23), (6, 8), (7, 0)	17^1, 37^1
179	(0, 0), (0, 48), (3, 30), (5, 16), (7, 0)	66^1, 67^1, 70^1, 71^1, 73^1, 74^1, 86^1
180	(0, 0), (0, 51), (1, 44), (7, 0)	52^1
181	(0, 0), (0, 48), (4, 24), (7, 0)	63^1, 68^1, 69^1, 85^1, 90^1, 94^1
182	(0, 0), (0, 48), (6, 0), (6, 12)	218^1, 219^1, 221^1, 222^1, 244^1
183	(0, 0), (0, 48), (3, 30), (6, 9), (7, 0)	65^1, 72^1, 95^1
184	(0, 0), (0, 48), (3, 30), (6, 0), (7, 2)	114^1, 117^1
185	(0, 0), (0, 48), (4, 0), (4, 24), (7, 3)	99^1
186	(0, 0), (0, 48), (3, 30), (6, 0), (6, 9), (7, 1)	80^1, 83^1, 100^1
187	(0, 0), (0, 48), (3, 30), (6, 9), (7, 0), (7, 1)	81^1, 84^1, 101^1
188	(0, 0), (0, 48), (3, 30), (6, 0), (7, 1), (7, 2)	116^1, 119^1
189	(0, 0), (0, 48), (3, 30), (7, 0), (7, 2)	115^1, 118^1
190	(0, 0), (0, 51), (3, 30), (7, 0)	107^1, 109^1, 112^1, 113^1, 140^1
191	(0, 0), (0, 48), (4, 24), (6, 9), (7, 0)	64^1
192	(0, 0), (0, 48), (4, 24), (6, 0), (6, 9), (7, 1)	79^1
193	(0, 0), (0, 48), (4, 24), (5, 17), (6, 9), (7, 0)	91^1, 120^1
194	(0, 0), (0, 48), (4, 24), (6, 9), (7, 0), (7, 1)	82^1
195	(0, 0), (0, 48), (4, 24), (5, 17), (6, 0), (7, 1)	127^1, 130^1
196	(0, 0), (0, 51), (3, 30), (6, 8), (7, 0)	108^1, 111^1
197	(0, 0), (0, 48), (4, 24), (5, 17), (7, 0), (7, 1)	128^1, 131^1
198	(0, 0), (0, 52), (3, 30), (7, 0)	106^1, 110^1

Ind.	2-face Vertices	Polytope$^{\text{Multiplicity}}$
199	(0, 0), (0, 48), (5, 18), (7, 0)	125^1, 129^1
200	(0, 0), (0, 51), (4, 23), (6, 8), (7, 0)	162^1, 163^1, 177^1, 178^1
201	(0, 0), (0, 48), (4, 24), (6, 10), (7, 0)	126^1
202	(0, 0), (0, 48), (4, 24), (6, 0), (7, 3)	168^1
203	(0, 0), (0, 48), (4, 24), (6, 0), (6, 10), (7, 1)	142^1
204	(0, 0), (0, 48), (4, 24), (6, 0), (6, 10), (7, 2)	149^1
205	(0, 0), (0, 52), (1, 45), (7, 0)	161^1, 164^1
206	(0, 0), (0, 51), (5, 16), (7, 0)	183^1, 185^1, 187^1, 189^1, 190^1, 191^1, 197^1
207	(0, 0), (0, 48), (4, 24), (6, 10), (7, 0), (7, 1)	143^1
208	(0, 0), (0, 48), (4, 24), (6, 0), (7, 2), (7, 3)	175^1
209	(0, 0), (0, 48), (4, 24), (6, 0), (6, 10), (7, 1), (7, 2)	154^1
210	(0, 0), (0, 52), (6, 8), (7, 0)	105^1
211	(0, 0), (0, 48), (5, 18), (6, 10), (7, 0)	141^1
212	(0, 0), (0, 48), (5, 18), (6, 0), (7, 2)	167^1
213	(0, 0), (0, 48), (5, 18), (6, 0), (6, 10), (7, 1)	148^1
214	(0, 0), (0, 48), (4, 24), (6, 0), (7, 1), (7, 3)	173^1
215	(0, 0), (0, 48), (4, 24), (6, 10), (7, 0), (7, 2)	151^1
216	(0, 0), (0, 51), (6, 9), (7, 0)	182^1, 188^1, 215^1, 227^1, 231^1, 234^1
217	(0, 0), (0, 51), (6, 0), (6, 9), (7, 1)	193^1, 195^1, 224^1, 233^1
218	(0, 0), (0, 48), (4, 24), (7, 0), (7, 3)	170^1, 180^1
219	(0, 0), (0, 48), (5, 18), (6, 10), (7, 0), (7, 1)	150^1
220	(0, 0), (0, 48), (5, 18), (6, 0), (7, 1), (7, 2)	172^1
221	(0, 0), (0, 51), (6, 9), (7, 0), (7, 1)	194^1, 196^1, 225^1, 230^1, 232^1, 236^1
222	(0, 0), (0, 48), (5, 18), (7, 0), (7, 2)	169^1
223	(0, 0), (0, 51), (7, 0), (7, 2)	228^1, 229^1, 235^1
224	(0, 0), (0, 48), (6, 12), (7, 0)	199^1
225	(0, 0), (0, 52), (6, 0), (6, 10)	283^1, 285^1
226	(0, 0), (0, 48), (6, 0), (6, 12), (7, 1)	203^1
227	(0, 0), (0, 48), (6, 0), (6, 12), (7, 2)	202^1
228	(0, 0), (0, 48), (6, 0), (6, 12), (7, 3)	201^1
229	(0, 0), (0, 52), (2, 38), (6, 8), (7, 0)	181^1, 192^1
230	(0, 0), (0, 48), (6, 12), (7, 0), (7, 1)	204^1
231	(0, 0), (0, 48), (6, 0), (6, 12), (7, 1), (7, 2)	210^1
232	(0, 0), (0, 48), (6, 0), (6, 12), (7, 2), (7, 3)	209^1
233	(0, 0), (0, 53), (6, 8), (7, 0)	186^1, 198^1
234	(0, 0), (0, 52), (3, 31), (6, 8), (7, 0)	184^1
235	(0, 0), (0, 48), (6, 12), (7, 0), (7, 2)	205^1
236	(0, 0), (0, 48), (6, 0), (6, 12), (7, 1), (7, 3)	214^1
237	(0, 0), (0, 48), (6, 0), (6, 12), (7, 2), (7, 4)	212^1
238	(0, 0), (0, 48), (6, 12), (7, 0), (7, 3)	206^1
239	(0, 0), (0, 48), (6, 0), (6, 12), (7, 1), (7, 4)	213^1
240	(0, 0), (0, 52), (4, 24), (7, 0)	240^1, 241^1, 242^1, 248^1, 249^1, 251^1, 252^1, 253^1, 254^1
241	(0, 0), (0, 48), (6, 12), (7, 0), (7, 4)	207^1, 220^1
242	(0, 0), (0, 48), (6, 0), (6, 12), (7, 1), (7, 5)	211^1, 223^1
243	(0, 0), (0, 48), (6, 12), (7, 0), (7, 5)	208^1, 226^1
244	(0, 0), (0, 48), (7, 0), (7, 6)	200^1, 237^1, 245^1
245	(0, 0), (0, 52), (4, 24), (6, 9), (7, 0)	239^1
246	(0, 0), (0, 52), (4, 24), (6, 0), (6, 9), (7, 1)	246^1

Ind.	2-face Vertices	Polytope$^{\text{Multiplicity}}$
247	(0, 0), (0, 54), (6, 8), (7, 0)	238^1
248	(0, 0), (0, 52), (5, 17), (6, 9), (7, 0)	250^1, 255^1
249	(0, 0), (0, 52), (5, 17), (6, 0), (7, 1)	263^1, 265^1
250	(0, 0), (0, 52), (4, 24), (6, 9), (7, 0), (7, 1)	247^1
251	(0, 0), (0, 52), (5, 17), (7, 0), (7, 1)	264^1, 266^1
252	(0, 0), (0, 52), (6, 10), (7, 0)	262^1, 273^1, 276^1
253	(0, 0), (0, 52), (6, 0), (6, 10), (7, 1)	267^1, 269^1, 277^1
254	(0, 0), (0, 52), (6, 10), (7, 0), (7, 1)	268^1, 274^1, 281^1
255	(0, 0), (0, 52), (6, 0), (6, 10), (7, 1), (7, 2)	271^1, 279^1
256	(0, 0), (0, 48), (8, 0)	243^1
257	(0, 0), (0, 54), (4, 24), (7, 0)	257^1, 258^1, 259^1
258	(0, 0), (0, 52), (6, 10), (7, 0), (7, 2)	270^1, 275^1, 280^1
259	(0, 0), (0, 52), (7, 0), (7, 3)	272^1, 278^1, 282^1, 284^1
260	(0, 0), (0, 54), (6, 9), (7, 0)	256^1
261	(0, 0), (0, 54), (6, 0), (6, 9), (7, 1)	260^1
262	(0, 0), (0, 54), (2, 40), (7, 0)	286^1, 287^1, 288^1, 289^1, 290^1
263	(0, 0), (0, 54), (6, 9), (7, 0), (7, 1)	261^1
264	(0, 0), (0, 56), (7, 0)	294^1, 295^1, 303^1, 304^1, 305^1, 307^1, 311^1, 312^1, 313^1, 314^1, 319^1, 320^1
265	(0, 0), (0, 54), (6, 0), (6, 12)	336^1, 337^1
266	(0, 0), (0, 54), (3, 33), (6, 9), (7, 0)	292^1, 293^1, 296^1
267	(0, 0), (0, 54), (3, 33), (6, 0), (7, 1)	297^1, 299^1
268	(0, 0), (0, 54), (3, 33), (7, 0), (7, 1)	298^1, 300^1
269	(0, 0), (0, 54), (4, 26), (6, 9), (7, 0)	291^1
270	(0, 0), (0, 54), (4, 26), (5, 18), (7, 0)	301^1, 302^1
271	(0, 0), (0, 54), (4, 26), (6, 10), (7, 0)	306^1
272	(0, 0), (0, 54), (4, 26), (6, 0), (7, 2)	316^1
273	(0, 0), (0, 54), (4, 26), (6, 0), (6, 10), (7, 1)	309^1
274	(0, 0), (0, 54), (4, 26), (6, 10), (7, 0), (7, 1)	310^1
275	(0, 0), (0, 54), (4, 26), (6, 0), (7, 1), (7, 2)	321^1
276	(0, 0), (0, 54), (5, 19), (6, 10), (7, 0)	308^1
277	(0, 0), (0, 54), (5, 19), (6, 0), (7, 1)	315^1
278	(0, 0), (0, 54), (4, 26), (7, 0), (7, 2)	318^1
279	(0, 0), (0, 57), (6, 9), (7, 0)	322^1, 323^1, 339^1, 341^1, 344^1, 345^1
280	(0, 0), (0, 54), (5, 19), (7, 0), (7, 1)	317^1
281	(0, 0), (0, 57), (7, 0), (7, 1)	342^1, 343^1, 346^1
282	(0, 0), (0, 54), (6, 12), (7, 0)	324^1
283	(0, 0), (0, 54), (6, 0), (6, 12), (7, 1)	327^1
284	(0, 0), (0, 54), (6, 0), (6, 12), (7, 2)	326^1
285	(0, 0), (0, 54), (6, 12), (7, 0), (7, 1)	328^1
286	(0, 0), (0, 54), (6, 0), (6, 12), (7, 1), (7, 2)	333^1
287	(0, 0), (0, 54), (6, 0), (6, 12), (7, 2), (7, 3)	332^1
288	(0, 0), (0, 54), (6, 12), (7, 0), (7, 2)	329^1
289	(0, 0), (0, 54), (6, 0), (6, 12), (7, 1), (7, 3)	335^1
290	(0, 0), (0, 54), (6, 12), (7, 0), (7, 3)	330^1
291	(0, 0), (0, 54), (6, 0), (6, 12), (7, 1), (7, 4)	334^1
292	(0, 0), (0, 54), (6, 12), (7, 0), (7, 4)	331^1, 338^1
293	(0, 0), (0, 54), (7, 0), (7, 5)	325^1, 340^1
294	(0, 0), (0, 58), (4, 26), (6, 9), (7, 0)	347^1

Ind.	2-face Vertices	Polytope$^{\text{Multiplicity}}$
295	(0, 0), (0, 58), (5, 18), (7, 0)	349^1, 350^1
296	(0, 0), (0, 58), (6, 10), (7, 0)	351^1, 355^1, 357^1
297	(0, 0), (0, 58), (6, 0), (6, 10), (7, 1)	352^1, 358^1
298	(0, 0), (0, 58), (6, 10), (7, 0), (7, 1)	353^1, 356^1, 360^1
299	(0, 0), (0, 58), (7, 0), (7, 2)	354^1, 359^1
300	(0, 0), (0, 60), (6, 9), (7, 0)	348^1
301	(0, 0), (0, 60), (3, 36), (7, 0)	361^1, 362^1
302	(0, 0), (0, 60), (6, 0), (6, 12)	376^1
303	(0, 0), (0, 60), (4, 28), (6, 10), (7, 0)	363^1
304	(0, 0), (0, 60), (4, 28), (6, 0), (7, 1)	365^1
305	(0, 0), (0, 60), (4, 28), (7, 0), (7, 1)	366^1
306	(0, 0), (0, 60), (5, 20), (7, 0)	364^1
307	(0, 0), (0, 63), (7, 0)	378^1, 379^1, 380^1
308	(0, 0), (0, 60), (6, 12), (7, 0)	367^1
309	(0, 0), (0, 60), (6, 0), (6, 12), (7, 1)	370^1
310	(0, 0), (0, 60), (6, 0), (6, 12), (7, 2)	369^1
311	(0, 0), (0, 60), (6, 12), (7, 0), (7, 1)	371^1
312	(0, 0), (0, 60), (6, 0), (6, 12), (7, 1), (7, 2)	374^1
313	(0, 0), (0, 60), (6, 12), (7, 0), (7, 2)	372^1
314	(0, 0), (0, 60), (6, 0), (6, 12), (7, 1), (7, 3)	375^1
315	(0, 0), (0, 60), (6, 12), (7, 0), (7, 3)	373^1
316	(0, 0), (0, 60), (7, 0), (7, 4)	368^1, 377^1
317	(0, 0), (0, 64), (6, 10), (7, 0)	381^1, 383^1, 384^1
318	(0, 0), (0, 64), (7, 0), (7, 1)	382^1, 385^1
319	(0, 0), (0, 66), (4, 30), (7, 0)	386^1
320	(0, 0), (0, 66), (6, 12), (7, 0)	387^1
321	(0, 0), (0, 66), (6, 0), (6, 12), (7, 1)	389^1
322	(0, 0), (0, 66), (6, 12), (7, 0), (7, 1)	390^1
323	(0, 0), (0, 66), (6, 0), (6, 12), (7, 1), (7, 2)	392^1
324	(0, 0), (0, 66), (6, 12), (7, 0), (7, 2)	391^1
325	(0, 0), (0, 66), (7, 0), (7, 3)	388^1
326	(0, 0), (0, 70), (7, 0)	393^1, 394^1
327	(0, 0), (0, 72), (6, 12), (7, 0)	395^1
328	(0, 0), (0, 72), (6, 0), (6, 12), (7, 1)	397^1
329	(0, 0), (0, 72), (6, 12), (7, 0), (7, 1)	398^1
330	(0, 0), (0, 72), (7, 0), (7, 2)	396^1
331	(0, 0), (0, 78), (6, 12), (7, 0)	399^1
332	(0, 0), (0, 78), (7, 0), (7, 1)	400^1
333	(0, 0), (0, 84), (7, 0)	401^1

Table 6: 2-faces and their associated fine triangulation counts.

Index	$N_{\mathrm{FT}}(f)$	Index	$N_{\mathrm{FT}}(f)$
1	1	48	1
2	1	49	104
3	2	50	156
4	1	51	454
5	1	52	734
6	3	53	13
7	1	54	522
8	1	55	204
9	4	56	378
10	2	57	609
11	4	58	91
12	6	59	1576
13	1	60	717
14	4	61	786
15	5	62	4713
16	10	63	2574
17	1	64	1048
18	1	65	2933
19	5	66	3782
20	6	67	7549
21	8	68	2183
22	15	69	9570
23	1	70	14303
24	5	71	7273
25	7	72	10660
26	18	73	21368
27	21	74	47256
28	24	75	7164
29	10	76	19611
30	13	77	37097
31	28	78	101547
32	53	79	141671
33	79	80	49488
34	36	81	1
35	84	82	1
36	1	83	668517487
37	31	84	41634159376
38	28	85	294384302208
39	71	86	13322475161785816128
40	98	87	94592566195943835168
41	120	88	126069338181924507924
42	210	89	503803582032732726348
43	1	90	671738109376976968464
44	11	91	12166488474600849404472
45	117	92	895307096508249363876
46	330	93	3578214261159145784376
47	300	94	4770952348212194379168

Index	$N_{\mathrm{FT}}(f)$
95	89695519146920262088884
96	6359080291811668807348
97	33889469562467768628048
98	240753501292063537182144
99	320915259993885481804920
100	1282874862704479693368840
101	1710499816939306257825120
102	35689780867280180104306320
103	12153775452208867396251648
104	11512840041723363475742752
105	46030516835118807378781377O
106	61374022446825076505041836O
107	14072716107444999145608986730
108	43617716994441606229762170 84
109	22033770063112369648900761958 8
110	21419025576195212867596970766238467 20
111	34376360956453265514768534597182975051
112	15661440184347840089475945884 88
113	20649676862322773372967486631694408653
114	513647299408750970166995022019722513065
115	219427689793456786330970142485762339 21
116	87185054841565916251350755121956995099 94
117	96057699234987274192179585917937585955 1
118	32847417358036312278828856760742445758 61
119	49526120403419750247226471528430111238 90
120	79763874407347302891324961214345388904 53
121	12770198302343953726214528884901187487821
122	22293466399359196009995730967433747703915 5
123	70021900950029197204323209389847206250 33
124	56254529912442735792694828930862 4
125	21228925419029859751587769892591860781257 14
126	369957440612680224228504864848982014446 00
127	12323487146862830448598046036223419117 1650
128	22056150631215304981670451568114985640383 36
129	23046834121805566441933376893576062512046 7
130	11883598769163207921113507864266738447454 50
131	916610532215873627293568757686152440030786257620
132	12633004099096493302485457721575498932676270
133	20211502582636107840692645946610 0344
134	553165236520732847552459951384736056410375 67
135	18916960442950301581867946695523044617211 0378
136	28524597590626821339804352228530137198821 9132
137	45974227262970142490687770143619457040808 5622
138	73590026243559933736305590374697548770032 2788
139	14204653084040660899635889091327296607597849236
140	14840820528504372979551146061884562878646820 7801
141	71013382942546383219278991025706539779545689 50
142	37678108480350859053071225484459321565649701165705 38
143	14021364958025323845105723360675504007888259 2797

Index	$N_{\mathrm{FT}}(f)$
144	6848908809913068419724599762888918383213850017 5
145	1644869646647467738658290770855062148998724761740 7
146	4096428267581828325753003863169546982479473905688 81
147	8844515720125631971983960629454666783786884083114227
148	3951227394633101028969524329889699996114576135274356
149	4381842088267347703951242550225680065358541289946074676607 0
150	2364780141012738037209761388888974184615451257261970688 5
151	5542148131091582909035536791786698280287749040508391558 48
152	2281125091576414350110391824973424924794307299666336031 14
153	1481285249517582825401097321768955899308234303358766230444360172
154	1317604818131502281182593022458372720738056632201502928680860 1
155	7613429829442893490996185072282000784812815006009127578015680597 75
156	2118333357726173135096265269058301757039957762135890854921160909363567263070393 25218
157	2664204057573020044051183130969508362676181386836131429604884971353842764915933 948664
158	1110137468623563156212875427034752962564764531635825876031810720103293849423088 9287224488
159	1826249995518171884386205887188921043975424027776866036806142677830689456535710 5417461073400378162113591 9
160	3100884329709028508401811442412985014492505432480548598109019734456483098934358 2016857091824504903741043 1
161	8455617594321372751499244401718158690684919074904442813397582794877298176371937 4601866474091938202685766 4
162	1270537283549510453091316685241261236128312254802543361520730531291365428088141 6863722951549155208866145 83
163	1060069479999828288974969873432956373932438594752816754724413780131807333510108 1071829853014990278945988 72
164	1227689761897000161813432099412645215178001126669846881242437373686826376511151 4477229504505431244261024944
165	1723141735396495453434239704236946251179787488685482117267040247962389444195491 9069300276897970202111310756
166	9575124318612956157364977106308706644131488812845210501617674584839606091589204 4413413801223883689952823513 6
167	1570029008392209025417008450316315369851424950774005048426208192503898567344591 7315302298885258901863389347 6
168	6584726404303514708112742576978928362006986215644998341243124752800439391125142 0429387253445162173830258023 8
169	2346417015219373289026897447476644707514162088591006736575512826443852643665245 2469801545723945163345761815 74
170	2207123221584617452485499098113409934511291633587986234122300265335276697720243 1812678210058684681901728453 7
171	2394431158284789576772823982016287421256548791995370831880474692578970854501826 4441819174148887442505828661 9
172	2118498141345070385742654891034365442864682296900393492697637213347331426991880 8095799373068134830324157585 28
173	3557124195630754428570875477356405708026125993748812041790997211051534330476704 1529960576415113958895887105 9
174	1137347736807361156132323752787270294859798910386519828331219547748655198857429 9979391084882981286309584932499

Index	$N_{\mathrm{FT}}(f)$
175	340443998478202267083162735622808016971894516010046073293925262074382384548551 888624268393078350155007400032 8
176	359892130975590577590910136819025207534268741934212514934991873133952047923967 091617497209902122663918899270797
177	304306027383353450417808234642511595822150240170790666345630788643280235328438 211697817786062405288824661842 92
178	419689719531268444347235170228802832387312069956979344353819098502937240831716 575135559853493197990471839764 2
179	143777387420846406438818645243499575078561712650865881052672811729755034547111 974811735894464055525646846906 26
180	515014206081446760827959088930808215090063758227372505273072568801804729850747 743355151836787092369482115336 7
181	354696425910318196674374810345204364892105434492826466716640320256076739989048 291551159059312076360479074251 91
182	107419635941662397951004368344710375001089490004054916948077630322738755546248 325919100527795535666102502252627 96
183	398878251227703190587590497075086062698287378483536572861863974908916932364572 118059452935083232088253630841 28
184	445191385475666715772072969156040703474538420468242408815499865645117484627043 726245444375875864079657114669 01
185	805791933922192498656800804212390208378236855930287886382262993737298741466494 612871708341964741821919307699 76
186	668625004001980278246289507640051919860727809005543017652941129867638973944238 798887698695794399963927030356 46
187	620111349687647253151576622324749036155946242713776575687998722541320099794673 596551638409991835789965385506 542
188	697344441569740984575713671019598337829989986514692273255307939900126651550825 081696069709758950801140036267 033
189	379435511535266834082383191217040613347304427797636026814113657884514255726100 318081507365768187837467207200 7563
190	260593651030747966442359050904818380092845586960617354786270911350598372269258 040805239233009927807526449818 185
191	942305478746865996036992268427766284835969827410805885787211685395833094333605 509897750482507611286831081976 84
192	199008314830876671917539978300134588141476766545438183626523616061061589979852 899913451227396993629617268075 307
193	712519893034183259765755505242156835258580645758994977264132751669960652967193 201667584930664973689521519439 011
194	182819412843840676930882413844181350312805424756942838611996446311533181365057 485533999030973384643803231148 2901
195	905880629098170106848659682384555868130399125192186300923440422953410410543588 293541906368421453786210497573 422
196	970010132623015424329921954733449643021233730300282514233945437393022986435519 742608521732513405567944567705 882
197	855269740047210195791865757197658391005323409092648515363651675396293388807307 687657062395887856541816083434 0675
198	696729428380011106264546414022532418743776346552032190050313020392136780476910 101995716569152712430033058171 031
199	169762372051503225453687815124253693401155152880535551836754859365082949284323 175890902046663214641510874317 5842

Index	$N_{\mathrm{FT}}(f)$
200	3578744781914997998509454705033810075358175134762852613178246461978343876346939979951026460293132786372096127582
201	1924334197500348978605728463527252256025939611540279381184006371136936281791454851600360105698736495766970856724
202	2256748516219472844021569969098663802408652614587370653026011286400305852724345224985170145663639606300106002972
203	2744532276973610878702668992324162298082673756677427878915072011216702911297592904994695059675443681381162756116
204	2691706548542309055718540686784460523416417149408815071231338740052133673286135722926254479779646023351928293657
205	2991220513007087905830469192079563092175173057610344864661371031102494838105548594616313839216231863095268535851
206	9263750816121557627292977216030162840346509044301294808946752616500372006420593347439416369371210760387093074357
207	2710631778288269860283600934734503683680533393077002397137200920483543836493432826415453933625425026068959540022 1
208	3151624031122865816446164058041113332922456039050054368836267325203284785972613994860436867322457741222982492832 6
209	4418339808316134490184949601234770050852552759235881326995231358774740714009067058312500730402319711619192299027 3
210	2229440994851266853277127983069172346174330104648771156239954361695773016285249337525529870885471157327633296626
211	5481328813630228543924715116931859166101985789315219523582511747254821386197253444166087598010701007084264352160
212	6498821357411500416147701357349751529555458792204731343698497795634833965018562067281349066531719588414478672841
213	9383916959531279883091611256780462148531367427569399705890755896247528266018744757559710617342971930246982361792
214	2947682001126397141037854999913345589456917376141444885187260878395083539620362555284043278226026629286076969191 91
215	2490028798048464008498893167427798313207010929544029006095761114349754882279330333362235006806954983271356185037 09
216	2208152884406692306450119673338171429163247647860586242821524444880628285532422626947092936097014684706929090252 1
217	3726090997097933308291641699863116597980371444539396071299425351999987418680399729360810639973334760706683731282 9
218	1265900039686752549416355397408875284753485362569637026051139731143672170854713838385780335800914365900778718345690
219	9247764002276421323134030532523317336377352345256278706323314708787950429575567907436209764868904182990897503235 0
220	1091316943613521354178156697949697123110682760798503459694084806656340614948413454063760431736869565626577096439 88
221	3502850617985339719644324155431863994745164666461616607511633571638921717341131716822156175377828391488420564498 21
222	6251978482212074284947491862441984314652040054147946188695880606095123092377314024598411784223671981812403617665 64
223	1933563217058395722640267723156943436355342613866732671650201752646018574691457991771127129135358416434031010167971
224	4571593641612101013207506784979123148903635311059582627529849480407667834778106030737361100832076948795246473288

Index	$N_{\mathrm{FT}}(f)$
225	293912022487449984994062487022417018374419881837499104439913293966428384388902 775502354809366467551914190952928703348
226	677548279427417428570530413761620690248296428292121561823921514281600074803642 808996173080457387530850352599622 26
227	575155862327394959937883008979961056084830828501067701611089968569039824593990 579443388719629004485748291310896 17
228	611351764491634419452766804603808598334973530708037275721101639303103500860350 993048183222909053534256921292963 75
229	197159007396279312885927194020350581030405054045753997318484891288215506116887 788444300271418752626215089186549364
230	739661547262945692279155014227277956481653747625897232013953535317703290821020 587416545820710517163010704773612 73
231	105906618210618521481050044457895052385984276558762929505661791362561455850324 793751555125395679053456382775049 0182
232	938442020344426296698745175365103478500422039841909518020456534478809843357319 779601593876531864454257077964896787
233	430305921029270496983574923453948301689174902915413952487890887155592934654665 401915090083605160336527194259856859
234	578103665955333801880398872438349898124578455979827107263507859927763714372682 093536007772024202376270932866964607
235	649631934887235732808710117992355752682697866215885929905017232239730485784648 750471391144984044194861359457764 7139
236	950308997237597215511352957132113784079318053323479448344192550754949301379403 403394085425605058418401593940250 1810
237	805729151889309299909749740836821647495450841397153317164740429562091764858013 809412316142823881400299651262118 9706
238	432296142990039602497912450995733648426090084437377363720097022057895229705586 565805758744063464708363719230566027 90
239	601129146027194192703919784783045948921531425101705736044031921778828771707442 979069294697232906721455393109453518 29
240	600387199860677447224806845473166813680049923565136174744319059954251756934778 905932771748627973993653474057392 7733
241	227866205213972249876393903573642957334185415259065944067484308878684251159960 815560635150153618504359631633432366616
242	369306325857895894948760680660803329174461574471293132943232275044625000123408 342218012980434325436847848118681001823
243	123514999200765926585108658999624804545276694604730226788572381438446891378170 459561969519539978248382283997838824 0799
244	379601938916232719370012854744022187625826160940379696616833662169618060321045 101669001225059668049889079325421735 4488
245	194931748920892200053348476082835706907612993483787368586153078265746823804418 145859156660821338545926143085283834 39
246	392425181281399604433733977686340963969818269542493885064951472272385086708147 106015914882115220722480049662713551 85
247	187556834318949610065248914986311088934253612628957749728100770635061302575692 864144111224513422834523975182309400 92
248	777589017166312676945389592704562064300881672076697913883652420386762046320056 672960859814096969653071178290966462 08
249	101450824162116490035374553767176240448925806280815464716957973268056966011759 508000952078696706704163831672004574 918

Index	$N_{\mathrm{FT}}(f)$
250	368965455901006284398606506724191141715456011930894608430118915963236548828482 645476303673124751717806259573196926330
251	973858011561900448373653146264955954613397572796567386878554692911627592997014 982132214516492394259687127520410674067
252	170301572038162244456956594361974368429315765638370518456297082995715527232921 754412935121822687444319258099393458481
253	240668104138494004519156635916094127502137676313919328516283946876432604843073 151157208674228726229839322852877399564
254	241913649670633914412572907622917905089626080173891940629758957794004783745178 475111736567825445245091393189325532373 9
255	401285327165998210804981572551100615059809334301107316189649457522956218271338 986184690359756736689129889605967456537 6
256	192530032998038909316811953519310022604753459296551163172603082669823437696766 296003397490495711812212553146958571757 94
257	825810871458304684532043940077981863794421444826055392391668558969376252618413 615755309136563354860220739378048350851
258	230377598841416772380845738611245110863058732152410809195643292012558539840664 205992987366971236501774491993203411365 06
259	100906997502092563329700956640979509541314697235867683235973371556082501199623 497362927779986329397373346615951849637717
260	220395055267953655957837869430299151392118899862450336475652700640921976356443 079347204116785070697829504065002355256 9
261	472861559046834980960501085361115087161858775592939210862672994267659487806758 278612884095570842792904097260949723408 6
262	314062151771460953216169904514068479712712832849969123082836212897456828722916 465252916294369030230839076786306188916 66
263	448374748435097152116682862407463279719558093825970772520600305721516663798165 461781421118151527797861815307042176121 64
264	445892162864331607261451155459356075903267153098914431766555207582747419210216 766637190399627372668533451676732583464255
265	181582454322026658945686758183172207227151824219895815317685157166496575213006 882869431414433462721083158019365296822107455 2
266	883296957739759754710185199946262042133707148651367901082018499721236398063091 103396441149446873327112604235097572465961 0
267	993575678898407592431735466616692795019425136536260276881765625001463011516475 535403448468191745927620905056236425322378 5
268	970008790381604116749788595065978225713466995368276068476514901499117632556146 997253203920639261795851101370360848118427 15
269	262714088854075410922348507724015019954615889064703766400170840447472688244093 068549950173898358511474239046061589583895 40
270	119850929762109429043679950902301445101039628864134060016803790243759872487547 287688052054359056082610656301238787287780947
271	366249765409576966652845400267047564108135752419518200467829760384720831071281 644878279605008581626216958889355284221834745
272	426173102190146521185320914086420867079975016064958217211346699415235935791449 965473218296455897921886087546438414091835403
273	606995131086276706554640363828800485966807789958755180587058933046269890752146 302986607790002204275656145746270121571037068
274	617473523995561021031409026811001890142930226870175329688322439420002025119002 360741797924746792971599745784666962261664 4073

Index	$N_{\mathrm{FT}}(f)$
275	731381053463065160742700942752770800121229560306156309278259824498180027234214601873039901174011160193302343352400369689030 7
276	125164013485357198500258850359434055371347883285889941356463361658230240447922728988916617755015713237439293750172952153718 8
277	146933629997586666111991378006603985838832141205554588272307462061391605863778311700317495909832838286896646432979584911427 3
278	430774197154541569097714258646959012028213792465127270991612172958768799794752909682482520893779395160900723350343041626603 25
279	490642833399275398594079422009871850124849048848670636000907926011610074555096661178162504848184449494123857234227333298272 5
280	152632977061331590093451405150374786189428805934790171600129005570603782159502148169797667189016266675806459744779556976976015
281	485711918990629364143376940360697295003624926483535918260674851999008066631800516677733741748149597152232697611365279890707 08
282	925150515521297957264946254953670359839577181643302776893334007508818168750669239843850173201160950092862968540919922300017 5
283	133505723557309094226483358565885255544888796744699273471737856250572222118139244475625688718405508175765937205381869817702 1
284	118302747168468284550910358139717222351278717292953554920362209730161647576663679064225253348512411415058564929770724222750 52
285	150314159651196977958079171101946974560652808008592454655026509142202382705509956170217957639828967418920823754505373205462851
286	222226440827867279238691076253809560476478510835288715018587147709062247659869578754825948520304212065566959206049065865394140
287	187401995787279652123728580706164700095582808100609835028054849091367312596009616727403527981522082596766576307218097667685685
288	140066293608612538667317451567309715529579036862322582179995947262050761900276843998089099703306342151127013197208177859308102 6
289	195664489823168458217596412350798431397217218836569531767811203981092417266252952481372305465749201606271664236194051755623981 0
290	919941196696769054574623736297833643747749454728532342877411283266224352008317982897403097058162443939444271981444124028552660 5
291	150067200117375353157477545251901340111732619935935500566178478099665284151261043110875168575277272086513802626642221331470627 56
292	586610459571293257687587703495401773641927185099113142312598414107118071386973597028647593674964744551057130060353084633345569 80
293	203460352087089471020175069718890956977694797569412973511372910946726932727679506737765191433143114175589191508898053641167614744
294	515792901038452981496920393544846315471784780377883590964834146725096906987003044806516358824141945979652293192979808607185045 8
295	133563495345846970504337541405439056576299812917036411979937541412835781681555354599521207553117653273581724888217215142157313 30
296	319333404090902730444021158361804327492673964160490039498879652201751234330928758114511005500705721395525618887278495277650314 93
297	538491290255904989677124467169765628156426768675526545341720929012533224857904716319875798717031842332490906683796699671518600 72
298	557668543091526783435913685301991217291284655734029421231997248653629955204377081058286121289919792156475445443928249355184202573
299	334821872434580062320174204617965859946602757939779307356294262850520906698212944280492415087073883524870706763355395757523370107 6

Index	$N_{\mathrm{FT}}(f)$
300	62046917243381443903898121179230310795826162169237774593074550124259529833777312859448502694454768413175148651075955789702812642 7
301	13059918803386420891765753830324522125630915234632231805248144253596166662958386847302237692270290930200249807840453737482146666503 06
302	29675094430930242185256420480550688462077752629683534736520635896119168949093031029238684153911163731056253839435728292857692320097 1010
303	80262015708839927144480512360867962965709843649221804564212953814470149304762954134364707230507860578977570992502944178577628342058820
304	95145202450745063450504532731424352481418386301071064798661495279115389797703106257513410610088633044312060952030776445594866373713492
305	10139221245248227114923732857274197339217196404629394349256475930465126237374810355384100099146172576888616605124080133842775635115779 65
306	19458134462078282463414871085864929680808080408754892008868242179401859548122576644856880443642742287813573225931407104512489177563068 8
307	64372188154684101737045003831196589683593718427831803727350963547356440338907173671328767246423340168640239360335162014432803076429586 1
308	17975178754628505575592857136456447198495222236602077449803991029860424548458975707920086317111488668213503518023961937222911659736837 97
309	26962028304754564320093312702015464599370410872731956847739378056567839039979584237346486985018168663016422208758696614266397822194546 30
310	22539027161373109302846220191943512466499616370536754316107400827369825509193291035327058436468958935477638556585526358009972170422298 58
311	31117127099953943921537466626154430209555854170700136896935944455878689273675165789213120686502032968948234721853181943986829837401028788
312	43698403083719545177516954423883440940966404919166303275432340550737341750575955642035119548448996376254866452506081479037868743857669093
313	28473402990495732703872597543193783916176886633549437471406658739444631051274875981221236454495526610251812698514468114179477121951454675 1
314	46828693737239883585148602425965802741192613573350631097188912777587288997618368279748520846995483212301666258433940302725308871203272591 0
315	22679668220477945436244202407080603561220795933814555257574198137573284174128862982132450645349679222044156928593120643389004199544711664 43
316	91980644952014017243986505969591157704944648987366836839115100635860123187428548260262715101618598517137350145051012524110478344558389613 98
317	70940995983130467794956880952777775565697104312271980092554340090658220089352602679997416914433406108545452425847528115937318344333847926 95
318	77033633426511134693210828880249856038911513446342011921728410912810318474123841140178191395893708737426406323247563168218727724386375992199
319	12523735335212990256228921801200163795676552403953472649249820398474876015900979694195943511981733237703741362064772040672695635852619629695851269
320	35928156038214119197633920238171303253865138903745824112620090488071804119016652960512870684653133015031519152342235389459506603249115958548632315 8
321	50748318508544113176350556385257077163862450010348644174334769621437328381613894606619145409329284721694748106316364672583117014739295157555895112 2
322	60622227954380524650187444214836887524349766528183626972687862704060040466692906104989902908006021450173415255689929761591135278746578154386673169 53
323	10074057044521874706925027959389299114980089750712901985421449620266598703942432508788043728582415671550066562258562104826610533394634614823347203741
324	67527472433661636399256619363267851765769272618635320772180184728224866769230312810856123097819154429432510330876883716929089827186335095818314223857

Index	$N_{\mathrm{FT}}(f)$
325	339574590691192987648440371863193433420063238127347709722489493295073912140579096795322207170406206340561361430896901807309959979284784009896752130617
326	931801653317154380405796079127491163178848775602726300987100894320086644389085463600516139586911636316099665808988346144688141670996126976005161734564
327	671896071479443252397624073058621675114328720807431944342706027946592414126042218015498125935902604150081917684336790108650398720951521058191343529753129551 77
328	113210456595614740437068942512303326906891868021424728575721375966415353629633382956194149938991328164835219354415298650981849534178679720671500166298005485 17
329	138845021020193556994074187950955048430352054677074458910170760273866806224575277174621395482524133493817296272985556392216634046306451241354398046726137774 6115
330	967479140887801179507910960898373130230792541742773312639671837127762260707754509594732410972390252725852029543611466053416786645706517989943484201582239494 5491
331	149196333495982099789073367656242335999549427842350684875132352692117501398648367033812341979527602029938305255085552123438377840312205847573978864336237627 87137466505452
332	190579248457371088732762966501194032554947719530488931023960632147240005995754129641652458369892654194081684660671193543235878863309607268397759585860509447 113636877998715
333	196228713200162411938978864181761876772101743989385885750500710865127833221308499197643973255639411782537399755819240889235207308904607213766931897164428188907008625400301874158061 1

References

[1] M. Demirtas, L. McAllister, and A. Rios-Tascon, "Bounding the Kreuzer-Skarke Landscape," *Fortsch. Phys.* **68** (2020) 2000086, arXiv:2008.01730 [hep-th].

[2] N. Gendler, N. MacFadden, L. McAllister, J. Moritz, R. Nally, A. Schachner, and M. Stillman, "Counting Calabi-Yau Threefolds," arXiv:2310.06820 [hep-th].

[3] A. Chandra, A. Constantin, C. S. Fraser-Taliente, T. R. Harvey, and A. Lukas, "Enumerating Calabi-Yau Manifolds: Placing bounds on the number of diffeomorphism classes in the Kreuzer-Skarke list," arXiv:2310.05909 [hep-th].

[4] V. V. Batyrev, "Dual Polyhedra and Mirror Symmetry for Calabi-Yau Hypersurfaces in Toric Varieties," *J. Alg. Geom.* **3** (1994) 493–545, arXiv:alg-geom/9310003.

[5] M. Kreuzer and H. Skarke, "Complete classification of reflexive polyhedra in four-dimensions," *Adv. Theor. Math. Phys.* **4** (2000) 1209–1230, arXiv:hep-th/0002240.

[6] M. Demirtas, A. Rios-Tascon, and L. McAllister, "CYTools: A Software Package for Analyzing Calabi-Yau Manifolds," arXiv:2211.03823 [hep-th].

[7] L. McAllister, J. Moritz, R. Nally, and A. Schachner, "Candidate de Sitter Vacua," arXiv:2406.13751 [hep-th].

[8] M. Demirtas, M. Kim, L. McAllister, J. Moritz, and A. Rios-Tascon, "Small Cosmological Constants in String Theory," *JHEP* **12** (2021) 136, arXiv:2107.09064 [hep-th].

[9] E. Sheridan, F. Carta, N. Gendler, M. Jain, D. J. E. Marsh, L. McAllister, N. Righi, K. K. Rogers, and A. Schachner, "Fuzzy axions and associated relics," 2024. https://arxiv.org/abs/2412.12012.

[10] C. T. C. Wall, "Classification problems in differential topology. V," *Invent. math.* **1** (1966) 355–374. https://doi.org/10.1007/BF01389738.

[11] N. MacFadden and E. Sheridan, "Calabi-Yau Threefolds from Vex Triangulations," 2025. https://arxiv.org/abs/2512.14817.

[12] P. Berglund and T. Hubsch, "A generalized construction of calabi-yau models and mirror symmetry," *SciPost Physics* **4** no. 2, (Feb., 2018) . http://dx.doi.org/10.21468/SciPostPhys.4.2.009.

[13] A. P. Braun, C. Long, L. McAllister, M. Stillman, and B. Sung, "The Hodge Numbers of Divisors of Calabi-Yau Threefold Hypersurfaces," arXiv:1712.04946 [hep-th].

[14] N. MacFadden, "Efficient Algorithm for Generating Homotopy Inequivalent Calabi-Yaus," arXiv:2309.10855 [hep-th].

[15] V. Batyrev and M. Kreuzer, "Integral Cohomology and Mirror Symmetry for Calabi-Yau 3-folds," arXiv:math/0505432 [math.AG].

[16] N. MacFadden, A. Schachner, and E. Sheridan, "The DNA of Calabi-Yau Hypersurfaces," arXiv:2405.08871 [hep-th].

[17] E. Welzl, *The Number of Triangulations on Planar Point Sets*, p. 1–4. Springer Berlin Heidelberg, 2006. http://dx.doi.org/10.1007/978-3-540-70904-6_1.

[18] E. Welzl (with J. Matoušek and P. Valtr). *Lattice triangulations*, Talk in Freie Univ. Berlin, November 13, 2006.

[19] E. E. Anclin, "An upper bound for the number of planar lattice triangulations," *Journal of Combinatorial Theory, Series A* **103** no. 2, (2003) 383–386.

[20] Kaibel, V. and Ziegler, G.M., *Counting Lattice Triangulations*, p. 277–308. London Mathematical Society Lecture Note Series. Cambridge University Press, 2003. arXiv:math/0211268 [math.CO].

[21] S. Yu. Orevkov, "Counting lattice triangulations: Fredholm equations in combinatorics," arXiv:2201.12827v2 [math.CO].

[22] S. Yu. Orevkov, "Asymptotics of the number of lattice triangulations of rectangles of width 4 and 5," arXiv:2412.17065 [math.CO].

[23] S. Yu. Orevkov, "Number of primitive lattice triangulations of some rectangles." https://www.math.univ-toulouse.fr/~orevkov/tr.html.

[24] M. Kreuzer and H. Skarke, "Reflexive polyhedra in 4 dimensions." http://hep.itp.tuwien.ac.at/%7Ekreuzer/CY/CYcy.html.

[25] S. Yu. Orevkov, "Data related to the paper 'Futher Bounding the Kreuzer-Skarke Landscape'." https://www.math.univ-toulouse.fr/~orevkov/KS-top401.html.